Cross-linked agarose-gelatine beads as a substrate for investigating biofilms of bacterial pathogens.

Dan Roizman[1§], Maren Herzog[1§], Arpita Nath[1], Nivetha Pachaimuthu[2], Ahmad Hujeirat[1], Benno Kuropka[3], Jens Rolff[1*], and Alexandro Rodríguez-Rojas[1,2*]

[1]Evolutionary Biology, Institut für Biologie, Freie Universität Berlin, Berlin, Germany.
[2]Small Animal Internal Medicine, Clinic for Small Animals, University of Veterinary Medicine, Vienna, Austria.
[3]Institute of Chemistry and Biochemistry, Freie Universität Berlin, Berlin, Germany.

[§]co-first authors
[*]Corresponding authors: alexandro.rojas@vetmeduni.ac.at, jens.rolff@fu-berlin.de

Abstract

Treating chronic bacterial infections is challenging, primarily due to the formation of biofilms, which render bacteria less susceptible and more recalcitrant to antimicrobials. Despite the significance of biofilms in natural and medical settings, *in vitro* models are very limited in replicating bacterial biofilm physiology during infection. To address this challenge, we have developed a new approach using a surface hydrogel to bring the *in vitro* studies of biofilms closer to *in vivo* situations. Our hydrogel substrate combines cross-linked agarose and gelatine. These biogel beads have several attractive properties, such as stability and autoclaving resistance, and can be rapidly colonised by bacterial pathogens when submerged in liquid culture. We tested this new substrate using three model bacterial pathogens: *E. coli, P. aeruginosa,* and *S. aureus*. The biofilms formed on the agarose-gelatine beads exhibited more robust growth than those on glass beads for all three species. Moreover, biofilms formed on the agarose-gelatine beads exhibited increased virulence factor production, as indicated by their distinct proteomic signatures. In addition, these beads also acted as a reservoir for biofilm quorum sensing molecules, such as acyl-homoserine lactone. These unique features closely resemble clinical situations, suggesting that our new substrate provides a more accurate representation of biofilm-associated infections than current approaches, such as glass beads. The advantages of our new substrate over current methods are clear, making it an up-and-coming model for studying biofilms of bacterial pathogens and offering a practical and convenient solution to the research community.

Introduction

Biofilms are microbial communities embedded in a self-produced matrix of extracellular gelatinous substances, facilitating cell-to-cell adhesion and surface attachment[1]. The formation of biofilms dates back approximately 3.5 billion years, as evidenced by early fossil records[2]. These microbial conglomerates are a shared phenotype across diverse microorganisms, including archaea and bacteria. Biofilms play a crucial role in microbial life and are essential for survival in various environments, particularly under stress[3]. Biofilms are ubiquitous and can be found in diverse habitats, from the mammalian gut to deep subsurface rocks[4]. It is a predominant lifestyle on Earth, and estimations say 40-80% of bacterial and archaeal cells can be considered biofilm[5]. For instance, it has even been proposed that the microlayer on the surfaces of both sea and freshwater bodies is a giant floating gelatinous biofilm[6].

Beyond their environmental significance, bacterial biofilms play a crucial role in various infectious diseases due to their impenetrable nature, which protects them from antimicrobial agents. This mode of bacterial growth is associated with several health-related issues, particularly chronic infections[7]. Notably, biofilms can survive in the presence of antibiotic concentrations that are much higher than those effective against their planktonic forms[8]. Health problems related to biofilms include infections associated with medical devices, persistent conditions, and malfunctioning medical equipment[9]. One well-known example of bacterial aggregates that significantly impact human health is dental plaque, an archetypal biofilm of complex microbial communities[10]. Oral biofilms are responsible for tooth decay and many other diseases, such as meningitis and endocarditis[11,12].

There is a substantial body of literature on bacterial biofilms. However, contradictory findings regarding biofilm physiology and antimicrobial strategies are prevalent, primarily due to the variability and artificial nature of the methodologies employed[13]. Theoretically, bacterial cells of all possible phenotypes, motile and sessile, exist in principle in every test tube with differing population ratios[14]. The planktonic growth mode predominates by at least two orders of magnitude under normal favourable laboratory conditions, combined with the relative ease of protocols, thereby being the focus for most clinical-related inquiries. However, the recalcitrant biofilm phenotype is often related to treatment failure[15]. The lack of consensus among the diverse biofilm cultivation and analysis techniques further complicates the issue[16]. For instance, the most widely used method for biofilm formation involves microtiter plates. Initially developed by Fletcher in 1977 for studying bacterial attachment, this technique has since been refined and used for quantifying biofilm biomass[17]. Several

methodologies exist to study biofilm formation under simulated natural conditions. One example is the modified Robbins device[18], which utilises a flow system to circulate liquid containing microorganisms[19]. Advances in fluorescence-based microscopy, such as confocal microscopy, have contributed significantly to our understanding of biofilm mechanisms when combined with later open[20] and closed flow chamber systems[19]. However, one common limitation of contemporary systems is that they are conducted on artificial surfaces, glass predominantly for microscopy purposes or metal or plastic coupons for other tests[21]. That is due to their fabrication using human-made materials like silicone, Teflon PTFE, polypropylene, titanium, or stainless steel. Some studies have shown that data extrapolated from research on biofilm bactericidal compounds conducted on abiotic surfaces, such as polycarbonate filters, may not be entirely applicable to biofilms growing on biotic surfaces, such as skin, due to ultrastructural[22] and physiological variations[23].

We were inspired by classic literature on 19th-century bacterial cultivation methods to pursue a new way to culture bacterial biofilms and explore alternative materials. Solid media, created by incorporating gelling agents into a liquid broth, is more suitable for separating and isolating microorganisms than liquid media[24]. In 1881, Robert Koch used gelatine to develop the first solid media. However, its susceptibility to bacterial digestion and melting temperature below 37°C compromised its practicality. These limitations led to the search for alternative agents. A suitable substitute resulted from Angelina Hesse, the wife of Walther Hesse, an associate of Koch, proposing using agar to prepare solid culture in 1887[25]. Agar offered many advantages over gelatine, including resistance to bacterial degradation and a higher melting temperature, making it more practical for microbial growth[26]. A decade after the standardisation of microbiological tests with Koch's postulates for identifying pathogens, he already recognised that colonies grown on agar are different phenotypically than those grown on gelatine, necessitating microscopic evaluation for confirmation; Apart from its stability, agar alone is not an accurate model for recapturing conditions closer to *in vivo* infections[27]. Nonetheless, procedures based on fast planktonic growth and single colony isolation at 37°C made gelatine obsolete, although it represented the closest proxy to a host environment[26]. Notably, bacterial pathogens discovered and described in that era still comprise most of the priority list 150 years later[28,29]. The rationale for this switch is two-fold: to equilibrate the focus between biofilm lifestyle compared and planktonic and to have better substrates mimicking organic surfaces that are more comparable to within-host scenarios.

Agarose, a purified derivative of agar, is still in use for the manufacturing of chromatography media for biomolecule purification, and this is done via cross-linking of its polysaccharide molecules[30,31]. This

crosslinking method has been a starting point for the work presented here. We sought to improve the biocompatibility of the substrate by incorporating gelatine. Our notion also stemmed from an emulsification method to produce bacteria embedded in agarose beads, which entails mineral oil and has been used as a slow delivery system for chronic infection models of *Pseudomonas aeruginosa* in rodents[32–34]. Furthermore, we were drawn to the advantages of the *in vitro* biofilm models that use glass beads as a substrate[35–37].

The ability of bacteria to attach to glass beads and grow, forming aggregates or biofilms, even before the term biofilm was coined, was well documented as early as in the forties of the last century in the works of Heukelekian and Heller in 1940[38] and by Zobell in 1943[39]. Building on previous research on biofilms, we develop a biological hydrogel-based substrate to enhance existing *in vitro* biofilm models for pathogenic bacteria. Our method combines and stabilises the advantages of the two classic substrates for bacterial growth in semisolid media: agar and gelatine. We also decided to take advantage of the protocols established for glass bead biofilm[40] model to shape our substrate as beads.

To study the biofilms of bacterial pathogens on the surface of crosslinked agarose-gelatine, we have chosen three well-established bacterial models. Specifically, we examined lab-adapted susceptible strains from three bacterial families belonging to the target group called ESKAPE[41], consistently listed as major concern pathogens[28,42]. Among these are two notable pathogenic bacteria, one gram-negative and one gram-positive: *Pseudomonas aeruginosa* (*P. aeruginosa*) and *Staphylococcus aureus* (*S. aureus*). We also employed the non-pathogenic *Escherichia coli* (*E. coli*) K-12 model. The latter is the best-established bacterial model system since its initial isolation a hundred years ago[43]. Although *E. coli* is generally considered a moderate biofilm former, its extensive study history allows for in-depth analysis due to all genetic toolboxes and the accuracy of modern databases such as EcoCyc[44].

Results

Generation of agarose-gelatine beads and properties. We focused on the two traditional substrates for semisolid media in microbiology: agarose and gelatin matrices. Due to their biological compatibility and low reactivity, we prepared a crosslinked polymer based on these materials to serve as a substrate. We first explored various concentrations of reagents and the crosslinking conditions to create a set of conditions that could be a starting point. The method we adopted, based on the catalytic crosslinking activity of divinyl sulphone, was first demonstrated by Porath, Låås & Janson[31], which, immediately following adaptation, showed great flexibility for diverse experiments in biofilm analysis. We attempted to develop optimal properties that would enable the fabrication of spherical beads. Combining 2% agarose and 2% gelatine produced the most favourable results for generating biogel spherical structures. Lower concentrations (ranging from 0.5 to 2%) led to easily deformable beads, while higher concentrations (ranging between 5 and 8%) solidified rapidly, posing handling challenges. These structured, spherical beads were formed by depositing desired volumes of the hot mixture of agarose-gelatine in ice-cold mineral oil, as illustrated in Fig. 1. Some preliminary experiments also confirmed that agarose-alone beads showed a lower biofilm growth than the combined beads. Gelatine-alone beads showed lower stiffness and deficient crosslinking compared to agarose or agarose-gelatine combination (see supplementary Fig. S1).

First, we used a multi-stepper pipette to dispense the hot mixture (4% agarose-gelatine each, at 60°C) into the ice-cold mineral oil container. The drops of agarose-gelatine assumed a spherical shape and gradually sank to the bottom of the mineral oil while solidifying due to the low temperature. This manual method is effective if a small number of beads are required. We also developed a high-throughput system to improve efficiency and streamline the process. This involved using a magnetic stirrer with heating to maintain the solution in a homogeneous liquid state and employing a peristaltic pump to achieve a continuous flow of drops, enabling us to create thousands of beads with consistent sizes in a short period. We estimate that the above system can generate between 60 to 75 beads per minute. By standardising the drop volume to approximately 40 µl by modulating the pump flow rate, we achieved an average diameter of approximately 4 mm, ensuring a highly reproducible procedure (see Fig. 1, Fig. S1, and Table S1 for further details). The coefficient of variation remained below 2% across five independent batches (Table S1). This approach enabled the bulk creation of agarose-gelatine beads (AGBs), a typical size of glass beads used for biofilm cultivation[45]. The crosslink of the beads using divinyl sulphone (DVS) is a method akin to fabricating Sepharose, a chromatographic matrix commonly used for biomolecule purification[30]. Our protocol also demonstrated high

reproducibility, as shown in Fig. S1, and the biogel showed significant stiffness and thermostability properties. Unlike its non-crosslinked counterpart, this biogel can withstand autoclaving without structural degradation.

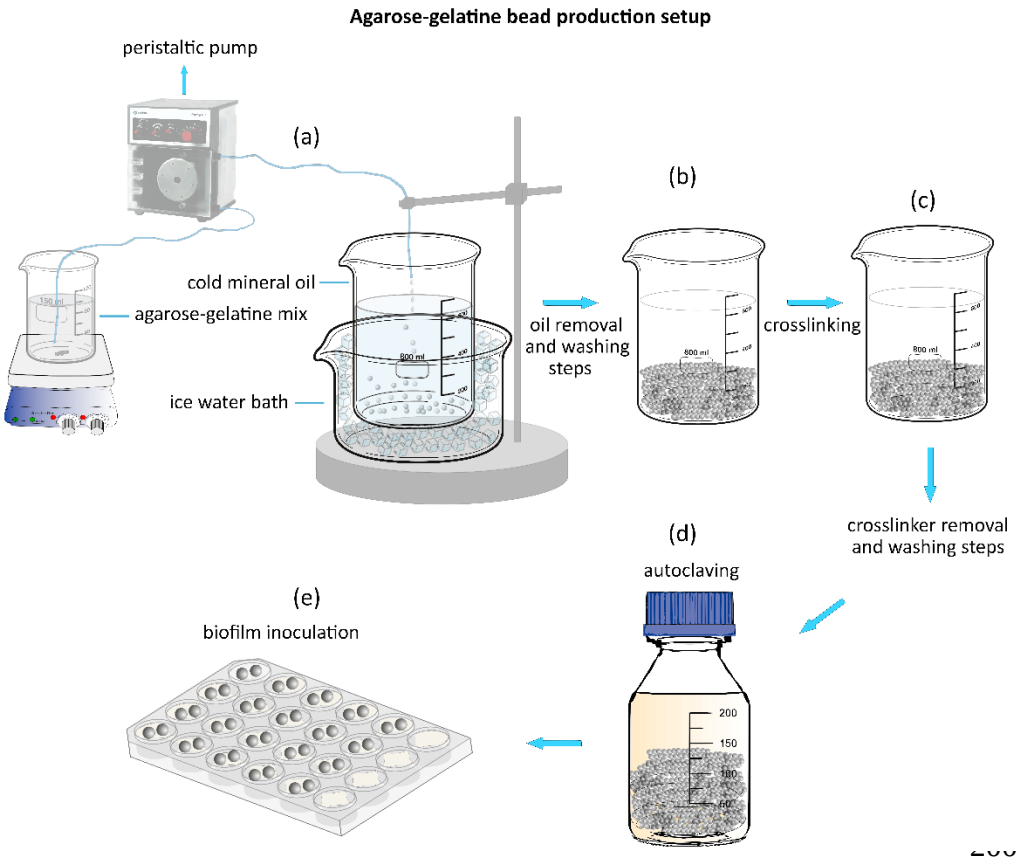

Fig. 1. A setup for generating crosslinked agarose-gelatine beads. In the initial step (a), a mixture of gelatine-agarose (2% each in distilled water) is prepared and placed on a magnetic stirrer with a hot plate to maintain liquidity. A peristaltic pump continuously pumps this solution, forming drops deposited into ice-cold mineral oil to create millimetre-scale beads. Subsequently (b), the mineral oil is removed, and washing steps, including detergent, are performed to eliminate oil residues. Following this (c), the beads undergo crosslinking using divinyl sulphone (DVS), with the crosslinker later removed through additional washing steps. After removal of the crosslinker, the beads are transferred to a bottle and autoclaved at 121°C for 15 minutes at 1 atmosphere (d). Once autoclaved, the beads can be stored for several months until use. In the final step (e), beads are transferred to a 24-well multiwell plate, where the chosen bacteria are inoculated, and the biofilm is established, as previously described. For additional details, see the Material and Methods section.

Next, we characterised the stability of the beads, which remained stable for at least five months after crosslinking and autoclaving. During the storage period in the culture medium, the AGBs did not change the aspect or diameter. The crosslinking not only provided the chemical stability to allow the beads to be autoclaved, but we also determined that the crosslinking significantly increased the beads' strength, manifested by a significant increase in stiffness as measured by Young's module of an atomic force microscope (Fig 2).

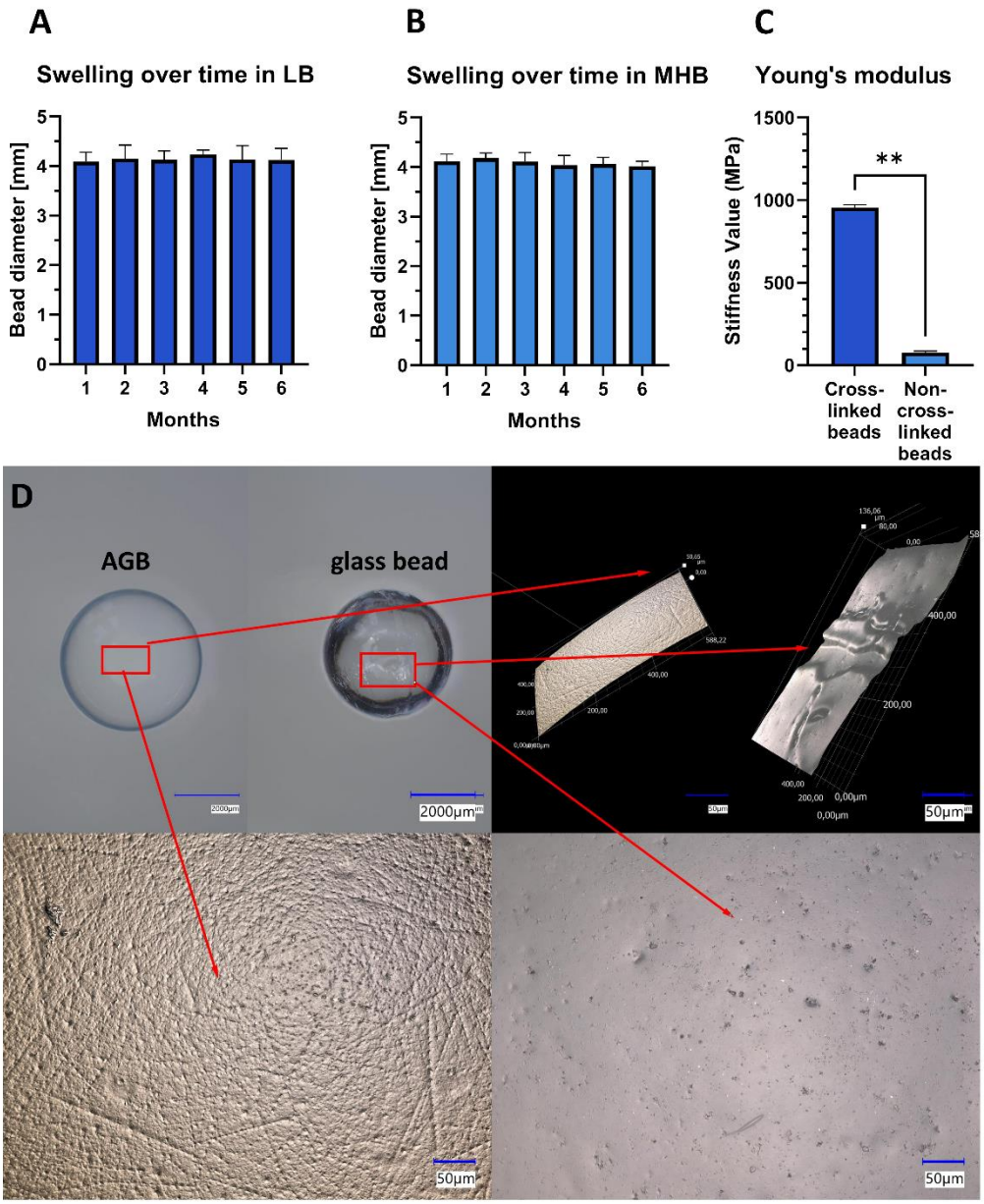

Fig. 2. Properties of agarose-gelatine beads. Swelling stability post-crosslinking and autoclaving for five months in two standard culture media: LB (A) and MHB (B). The bars represent the mean of 5 beads (N=5), and the error bars represent the standard deviation. The crosslinking significantly increased the stiffness of the beads as measured via Young's module of an atomic force microscope (C). We performed a student's t-test, and the four Asterix indicate that the *p*-values were below 0.0001. Comparative surface view of AGB and glass bead acquired with a Keyence VHX-X1 microscope.

Escherichia coli, _Pseudomonas aeruginosa_ and _Staphylococcus aureus_ form robust biofilms on the Agarose-gelatine beads.

E. coli, *P. aeruginosa,* and *S. aureus* all formed biofilms on the surface of the AGBs, which were compared to glass beads. Quantification of bacterial biofilm cells by counting colony-forming units per millilitre (CFU/ml) revealed significantly more biomass for bacterial cells grown on AGBs than on glass beads for all strains (Fig. 3). We measured these values during the maturation process of biofilm at 24

and 48 hours. The number of CFUs for all three bacterial species was significantly higher for AGBs compared to glass beads at 24 and 48 hours. In preliminary experiments, we observed a higher variation of the bacterial count coming from the AGBs than from the glass beads. We suspected the heterogeneity was due to protocol limitations, so we modified the bacterial recovery protocol by incorporating mechanical and chemical methods. The method included using some enzymes to digest the extracellular matrix (see M&M and SM). We fundamentally used DNase I and papain, which helped in better dispersion and a good level of single cells in suspension, which is crucial for a satisfactory enumeration.

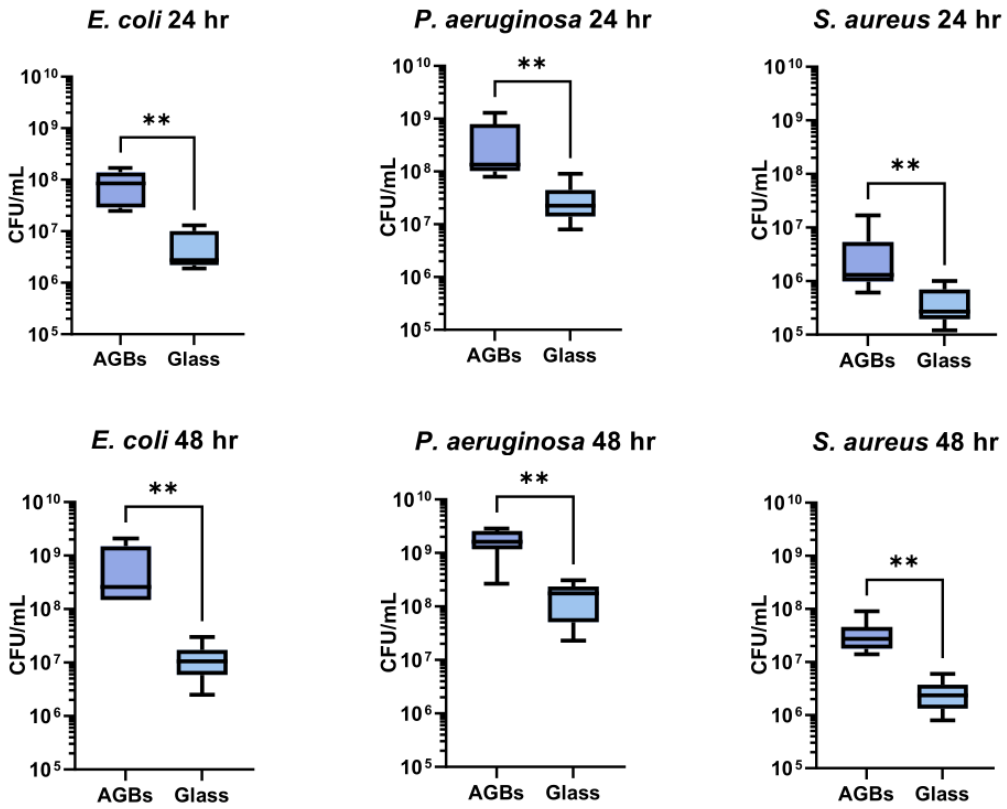

Fig. 3. Comparative biofilm formation of *E. coli*, *P. aeruginosa*, and *S. aureus* in agarose-gelatine beads and glass after 24 and 48 hours. Boxplots of bacterial count from six biofilm-containing beads for each species grown on the surface of the beads at 24 and 48 hours (N=6). The samples were compared via the Wilcoxon-Mann-Whitney test, and the two Asterix indicate that the *p*-values were below $p<0.01$.

Agarose-gelatine beads are compatible with scanning electron microscopy and live fluorescence microscopy.

The transparency of agarose is particularly advantageous for live fluorescence microscopy, enabling clear visualisation of bacterial cells in real-time without interference. Furthermore, the biocompatibility of agarose-gelatine ensures that the bacterial cells remain viable and maintain their

physiological states, leading to more reliable and relevant results in biofilm research. As a proof of principle, we tested a fluorescent strain of *E. coli* on the surface of the AGBs using fluorescence confocal microscopy (Fig. 4A and 4B).

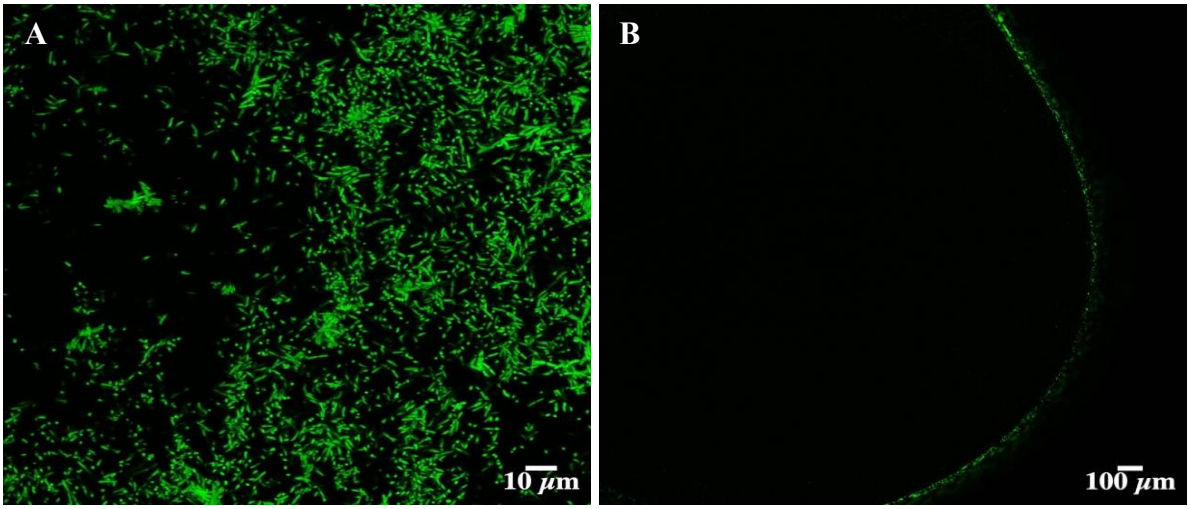

Fig. 4. Visualization of AGB biofilm formed by GFP-labelled *E. coli* cells using confocal laser scanning microscopy. Sections of the AGBs were allowed to mature into a biofilm over 48 hours. (A) A Z-stack comprising 29 images revealing a surface section of the AGB densely covered with an intact *E. coli* biofilm. (B) A single image extracted from the Z-stack displayed an AGB cross-section uniformly coated with *E. coli* biofilm.

Another relevant technique to study bacterial biofilms is scanning electron microscopy (SEM). Due to their hydrogel nature and spherical shape, the AGBs required special treatment (see M&M section) to fix, dehydrate, and keep the integrity of the structure of the beads and preserve the bacterial biofilm. The best results were obtained by drying all the beads with the critical point dryer. Then, we could perform scanning electron microscopy of *P. aeruginosa* and *S. aureus* biofilms (Fig. 5). The gelatine component offers a suitable texture that facilitates sample preparation and enhances electron imaging, capturing fine details of biofilm architecture.

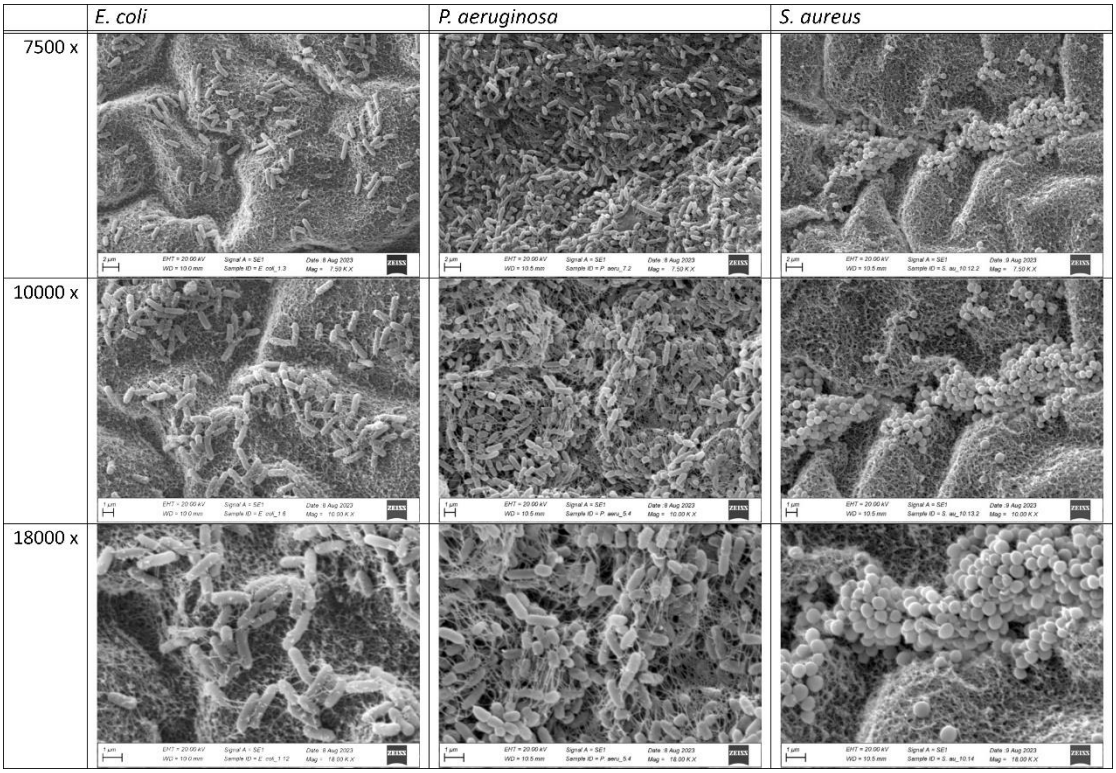

Fig. 5. Scanning electron microscopy characterisation of bacterial biofilms grown on agarose-gelatine beads. Biofilms on the surface of an AGB after 48 hours of cultivation for *E. coli*, *S. aureus* and *P. aeruginosa* at different magnifications.

Quantitative proteomics (LC-MS) shows that biofilms on Agarose-Gelatine beads and glass beads are different.

A pertinent piece of information to understand the difference between bacterial biofilms growing on AGBs and other substrates such as glass is the evaluation of gene expression and bacterial physiological changes. For this purpose, we employed label-free quantitative proteomics. All three bacterial species—*E. coli*, *P. aeruginosa*, and *S. aureus*—displayed distinct protein expression profiles in biofilms grown on agarose-gelatine beads (AGBs) compared to glass beads. We used a modified protocol developed *ad doc* for this study with some variations from previous works[46,47]. We have identified and quantified 1113 proteins for *E. coli*, 1500 proteins for *P. aeruginosa,* and 1251 proteins for *aureus* (Supplementary Table 1). Proteins with at least a 2-fold change in their relative intensity between glass beads vs. agarose-gelatine beads and an FDR-adjusted *p*-value < 0.05 were considered significantly changed. Remarkably, we observed that some important virulence factors for *P. aeruginosa* and *S. aureus* showed significant changes in their abundance, probably indicating a difference in surface sensing due to chemical composition (Fig. 6).

In biofilms of the *E. coli*, the 50S ribosomal subunit protein L35 (RpmI) was the protein with the most robust significant increase in relative abundance when grown on AGBs compared to glass beads (log2

fold change (log2FC) = 2.5). The small 30S ribosomal subunit S16 (RpsP) showed moderate upregulation on AGBs (log2FC = 1.1). The ribosomal silencing factor (RsfS) was also upregulated on AGBs (log2FC = 2.1). RsfS is known to be expressed when cells are more slowly growing; its role is to inhibit and modulate translation, and it indicates that much of the population on AGBs is in the mature quasi-stationary phase, which is expected for mature biofilms[48]. On glass beads, on the other hand, there is an even more distinct upregulation of 50S ribosomal subunits RpmH and RplU, or subunits L34 and L21 (Fig. 6) as for *E. coli*; at log2FC = -5.2, RpmH was the most differentially abundant protein. Apart from this striking difference in ribosomal structural content on glass beads, several other ribosome-associated proteins were upregulated: RsmH, Sra, YgaM and Rmf. RsmH is 16S-rRNA-m4C1402-methyltransferase, ubiquitous in bacteria and eukaryotic organelles; it facilitates a modification of the ribosomal P translation initiation site, allowing different codon usage for more efficient ribosome biogenesis[49]. The physiological roles of Sra and YgaM are less known, but they are considered regulatory[48]. The former tends to bind active 70S Ribosomes during the stationary phase and maturation, and the latter provides ribosomes with an anchoring point to the membrane. Rmf, or Ribosome modulation factor, is essential for the reversible formation of 70S-90S-100S Ribosome Dimers in gammaproteobacteria[48]. On glass beads, there is also a higher expression of NusA (log2FC = 2.9), which acts as a transcription terminator factor and a chaperone of rRNA, increasing their numbers; NusA is expressed following stress such as cold shock[50]. Overall, we see different ways of maturing and diversifying the ribosomes in size, structure, activity, and biogenesis. This trend is evident in all three strains, with potentially more regulatory shifts and stress response adaptations in biofilms on glass beads, indicating that glass beads are a more stressful substrate. Data also shows a notable change in cell division via Z-Ring formation through FtsZ polymerisation, an essential process for cell elongation and division. Notably, ZipA, which anchors FtsZ to the membrane, was significantly more abundant (log2FC = 2.2) on AGBs, contrasting with the upregulation of ZapA (log2FC) = -2.1) on glass beads, which influences cell division dynamics[51].

For *P. aeruginosa*, important virulence factors were more abundant in AGBs than in glass beads. This is the case of elastase (LasB), which showed the most prominent change in relative abundance (log2FC = 5.1). Elastase is regulated by the LasR/LasI quorum-sensing system, indicating vigorous virulence factor activity in biofilms grown on AGBs[52]. The second most prominent protein is PrpL (log2FC = 3.2), termed Protease IV or lysyl-endopeptidase, which can cleave fibrinogen and disturb the activity of the immune system[53]. We see more abundance of many other proteins in the biosynthesis pathway of pyoverdine on AGBs, most prominently for four of them: PvdA, PvdJ, PvdD and PvdL and then PvdF on glass beads; these are involved in different stages of pyoverdine production, a process that involves

the products of over 20 genes[54]. The primary function of pyoverdine is iron chelation from host cells, which are involved in *in vivo* infections. The primary function of pyoverdine is iron chelation from host cells, which are involved in *in vivo* infections. Additional significant differentially upregulated proteins in AGBs related to virulence detected in our analysis were the aminopeptidase Lap, also termed PaAP, which helps cleave extracellular proteins[53] and PhzM, involved in pyocyanin biosynthesis. The only virulence-related upregulated protein on glass beads was AmrZ, also known as AlgZ (log2FC = 3.0), which is an important transcription factor that regulates Alginate production and motility[55,56] while repressing other factors such as psl and is considered a step between colonisation before chronic infection as it has also been seen *in vivo* by *P. aeruginosa* biofilms[57].

Conversely, components of the Sec translocon system, such as YajC (-4.4 log2FC) and SecF (-2.5 log2FC), were less abundant in AGBs, indicating reduced protein export and altered membrane dynamics[58]. Our findings also point to the need for further investigation into the role of the Sec translocon in biofilm formation. The Sec translocon system components, such as YajC (-4.4 log2FC) and SecF (-2.5 log2FC), were less abundant in AGBs, indicating reduced protein export and altered membrane dynamics. It is expected that in mature biofilms, bacteria slow the metabolism, decreasing the protein secretion level. Unfortunately, we could not find research addressing this topic and its biological meaning in the literature. The second and third most abundant proteins on glass beads are uncharacterised PA0049 and PA5305 (with log2FC = -4.2 and -3.7, respectively). PA0049 is under the stringent redundant response regulator DksA in *P. aeruginosa*[59]. While DksA minor upregulation of proteins could be detected, it was below our significance threshold of log2FC = 1.0. A large proportion of proteins are probable, putative, uncharacterised or hypothetical (termed only with a locus tag and no gene name) for *P. aeruginosa* (18 of the 55 abundant proteins on AGBs and 113 of the 240 on glass beads, between 30-50%), detected to be above our specified threshold for significance change; *S. aureus* showed a similar trend. Thus, a comparative analysis is more intricate for both organisms relative to *E. coli*.

In *S. aureus* biofilms, we observe a similar trend as in *P. aeruginosa* regarding the higher level of virulence factors in AGBs compared to glass beads. However, the response of *S. aureus* is more complex due to the higher number of differentially expressed proteins for both substrates (247 Proteins on AGBs and 297 on glass beads). *S. aureus* showed about twice the number of proteins with altered levels compared to *E. coli* and *P. aeruginosa*. These results indicate that different species have differential responses in the class of proteins and the number of genes that respond to the type of surface where the biofilms develop. DeoC was the highest expressed protein on AGBs (log2FC = 5.0);

439 in bacteria, it is usually part of the inducible *deo* operon, which enables the metabolism of exogenous
440 nucleosides[60]. DeoC, or deoxyribose phosphate aldolase, is a duplicated gene in *S. aureus*[61]. Both
441 copies are highly upregulated on AGBs (log2FC = 2.5), and so are other genes in this operon, DeoB and
442 DeoD. The second most abundant protein on AGBs was MsrB (4.9 log2FC), a methionine sulfoxide
443 reductase that protects against oxidative stress and is a marker of a mature biofilm[62]. DltC was next
444 on the list, as it is critical in teichoic acid biosynthesis, cell envelope overall charge, and virulence[63].
445 The most abundant protein on glass beads was the most abundant in any condition in our analysis (8.0
446 log2FC), named SAOUHSC_02161, which is an MHC class II analogue protein of unknown function; it
447 is thought to be an attachment protein under the SaeRS two-component system regulon[64].
448
449 Several transcription factors and additional regulators were significantly increased on glass: SarR,
450 FapR, Rex, RecX, MsrR, and Spx; while on AGBs, seven other transcription factors are upregulated:
451 ArcR, NusB, NusG, CodY, NusA, SrrA, RsbW and VraR. SarR downregulates the expression of SarA,
452 which usually activates the agr operon quorum sensing system, leading to increased production of
453 exotoxins required for virulence[65]; FapR is a regulator of membrane lipid biosynthesis and lipid
454 homeostasis[66], Rex is a redox-responsive repressor that is activated by the ratios of NADH:NAD in the
455 cells; its regulon enzymes are involved in many metabolic pathways[67]. RecX is an anti-recombinase as
456 it inhibits RecA under accumulated DNA damage[68]. MsrR regulates the homeostasis of the cell
457 envelope and virulence factor production by structural means, known to be in abundance in antibiotic-
458 tolerant cells[69]; Spx is a global effector that accumulates in the cell during various stresses and
459 regulates a multitude of pathways, most notably thioredoxin in cells by a unique mechanism[70]. In
460 biofilms on AGBs, the most abundant regulator is ArcR, which is critical for anaerobic metabolism,
461 mainly allowing the metabolism of arginine over sugars[71]. Nus is an accessory protein forming a
462 complex with RNA polymerase enhancing bacterial rRNA transcription and synthesis[72]. CodY is a
463 regulator that affects the *agr* virulence system depending on population density and nutrient
464 scarcity[73]. SrrA is part of the two-component system SrrAB that increases virulence factor production
465 through *agr* at low oxygen levels[65]; RsbW is a serine-protein kinase that acts as an anti-sigma factor to
466 SigB, inhibiting transcription after binding[74]; and VraR is part of the two-component system VraSR,
467 which is upregulated in response to cell-wall damage affecting peptidoglycan homeostasis[75].
468
469 Regarding other pathways leading to virulence factor abundance, we see a differential upregulation
470 on glass beads, such as the biosynthesis pathway of staphyloxanthin: AldH1, CrtM, CrtP, and CrtN.
471 Additional virulence factors more abundant on glass beads are two fibrinogen-binding proteins
472 (SAOUHSC_01114, SAOUHSC_01110), Immunoglobulin binding Sbi and two uncharacterised

Leukocidin-like proteins (SAOUHSC_02241, SAOUHSC_02243). Several subunits of the Phenol-Soluble Modulin are upregulated (psmA1/A2 and psmA4). ClfA, or the clumping factor that facilitates the clumping of cells and thus defence from phagocytosis, is a more abundant component of the gamma and delta haemolysins. There is a notable abundance of extracellular active enzymes such as serine protease SplE and Coagulase (SAOUHSC_00192) and a plethora of known staphylococcal antigens (IsaB, SsA2, SsL10, SsaA). On AGBs, we can detect the upregulation of virulence-promoting factors, such as TraP and LuxS. TraP is involved in the upregulation of the *agr* operon in a cell density-dependent manner[76], LuxS is the enzyme which produces autoinducer-2 molecule, which in turn results in enhanced biofilm phenotypes[77]; Notable enzymes involved in pathogenesis were more abundant on AGBs: Lipase 1 or LipA, Catalase katA. The type VII secretion system components, EsxA and EsaG, are important for intracellular infection of the host[78].

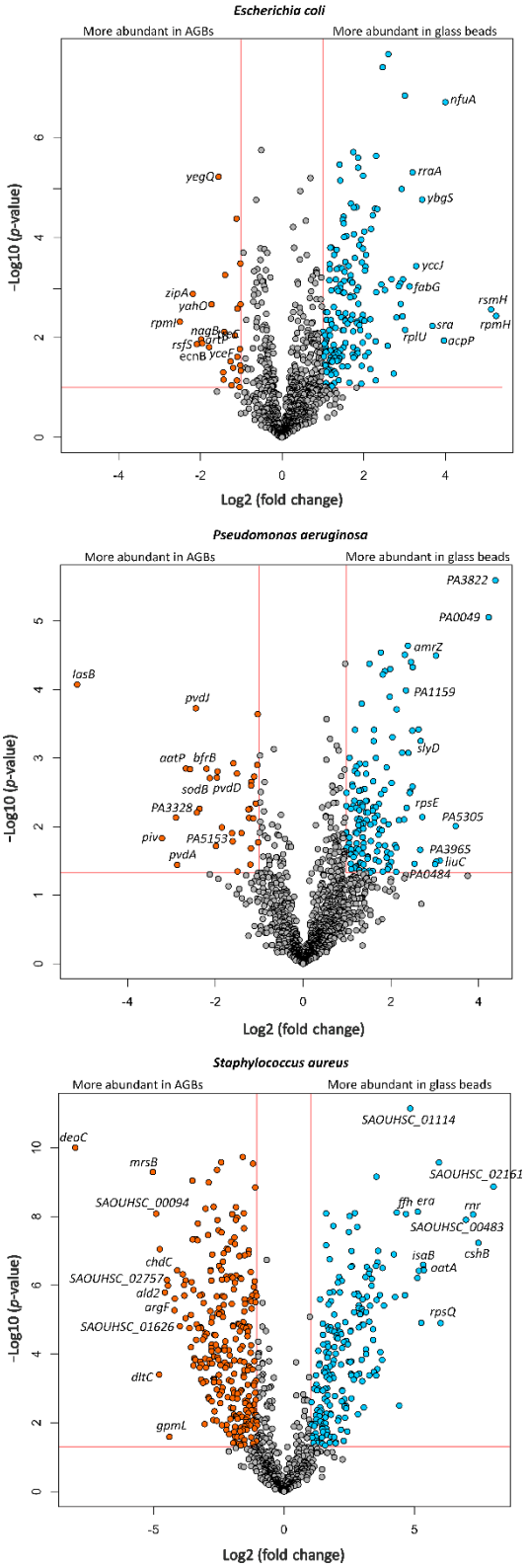

Fig. 6. Comparison of relative protein abundance between agarose-gelatine beads and glass beads for bacterial biofilms of *E. coli*, *P. aeruginosa*, and *S. aureus*. Volcano plots show relative protein intensity changes between AGBs and glass beads measured by LC-MS and label-free quantification. Orange dots denote proteins significantly more abundant in AGB biofilms, while blue dots indicate proteins more abundant in glass beads biofilms. Proteins are considered significantly changed if they show at least a 2-fold change in their relative abundance (log2 fold change >1 or <-1) with an FDR adjusted *p*-value < 0.05, as indicated by the orange lines.

The AGBs are suitable for the detection of biofilm-deficient strains.

Our model system presents a valuable tool for detecting or screening genes and conditions influencing biofilm formation. To validate this concept and assess the capability of Agarose Gel Biofilms (AGBs) to detect variations in biofilm formation, we studied two bacterial strains known for their deficiencies in biofilm formation. Early biofilm research established that type I fimbriae, produced by the *fim* operon, are crucial for forming submerged biofilms. Furthermore, type I pili, which include the mannose-specific adhesin FimH, are essential for the initial attachment to surfaces[79]. In previous years, we reported that disrupting the *pfpI* gene in *P. aeruginosa* impairs the bacterium's ability to form biofilms[80]. When we cultivated both mutant strains in AGBs and compared them with their respective parental wild-type strains, we observed a significant decrease in biofilm formation (Fig. 7). This finding indicates that our AGB system is adequate for detecting differences in biofilm formation between strains.

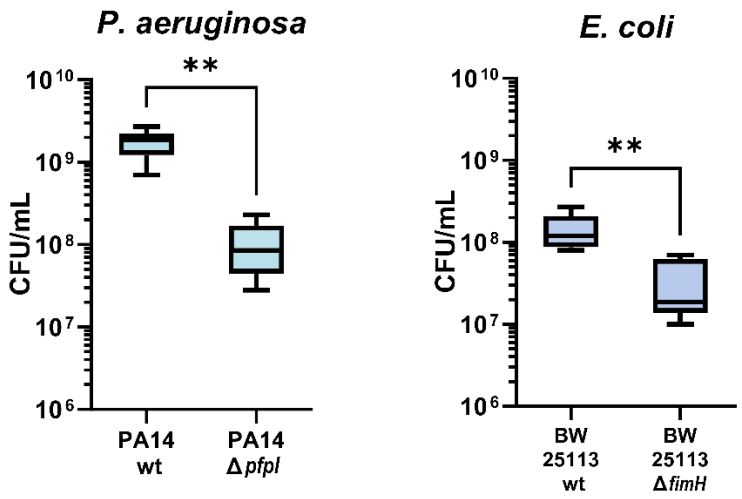

Fig. 7. Comparative biofilm formation of two biofilm deficient strains of *E. coli* (Δ*fimH*) and *P. aeruginosa* (Δ*pfpI*) on AGBs after 24 and 48 hours. Boxplots of bacterial count from biofilms of *E. coli* and *P. aeruginosa* mutants compared to their respective parental wild-type strains (N=6). The samples were compared via the Wilcoxon-Mann-Whitney test, and the two Asterix indicate that the *p*-values were below $p<0.01$. The Boxes extend from the 25 to the 75 percentiles, and the whiskers represent minimal and maximal values, with the middle line representing the mean.

Chemical modification of agarose-gelatine beads is a useful strategy for investigating anti-biofilm compounds.

One of the significant advantages of crosslinked agarose is its potential for conjugating diverse chemical compounds to its surface. This feature benefits our biofilm model and has practical implications for investigating antibiofilm compounds aimed at surface protection—a crucial aspect of biofilm research. As a proof of concept, we selected melittin, an antimicrobial peptide known for its anti-biofilm properties. Using the cyanogen bromide method, we adapted the protocol described by

March *et al.* to couple melittin to agarose-gelatine beads[81]. We used beads and bovine serum albumin (BSA) as a negative control.

Cultivating biofilms of our three bacterial models on melittin-decorated AGBs revealed a dramatic decrease in bacterial attachment to the bead surfaces compared to untreated and BSA-coupled beads. For all three bacterial species—*E. coli*, *P. aeruginosa*, and *S. aureus*—the number of biofilm-forming bacteria was reduced by 4 to 5 orders of magnitude compared to the controls (Fig. 8). Biofilms grown on BSA-coupled beads exhibited the highest biofilm formation, suggesting that the chemicals used for protein coupling to the AGBs were not responsible for the observed biofilm inhibition.

Notably, the final viability of planktonic bacteria did not differ in the wells where the bacterial species were incubated, indicating that the observed effects were specific to biofilm formation.

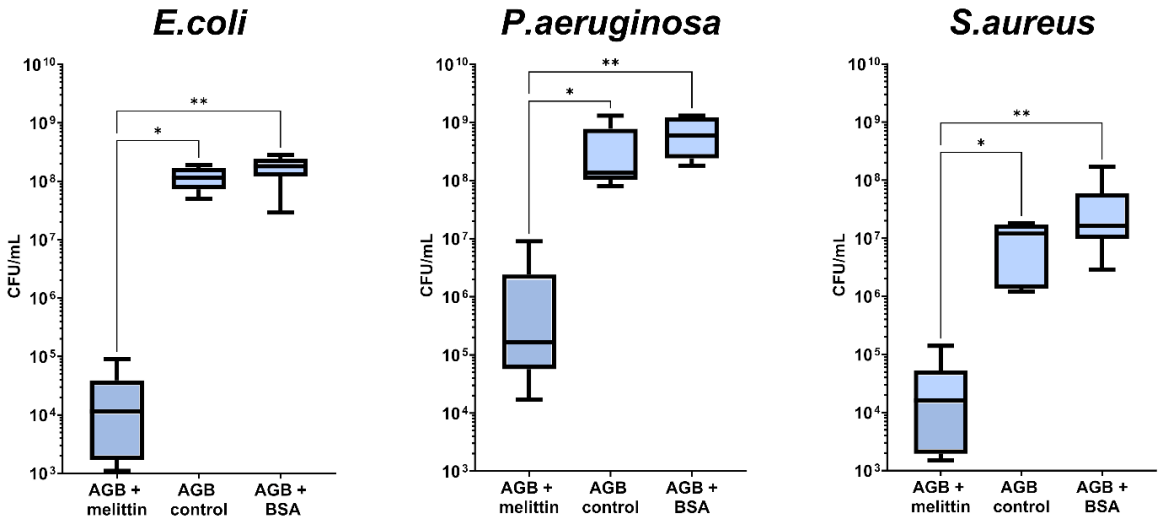

Fig. 8. Comparative biofilm formation of *E. coli* and *P. aeruginosa* and *S. aureus* on melittin-decorated agarose-gelatine beads after 48 hours of incubation. Boxplots of bacterial counts from biofilms attached to melittin-coupled, uncoupled, and BSA-coupled after 48 hours of incubation (N=6). The samples were compared via the Wilcoxon-Mann-Whitney test. One asterisk represents $p < 0.05$, and two asterisk for $p<0.01$. The Boxes extend from the 25 to the 75 percentiles, and the whiskers represent minimal and maximal values, with the middle line representing the mean.

Agarose-gelatine bead biofilms can be quantified with crystal violet assay.

A popular and convenient system to quantify bacterial biofilms is determining the crystal violet stain retained by biofilms[82]. We have tested this possibility with our AGBs and compared the performance of the crystal violet staining with biofilm grown in glass beads. Initially, using an adapted standard protocol for glass beads, the beads accumulated an intensive background of crystal violet compared to the glass beads. Therefore, we introduced some modifications in the protocol to control this issue. Following some introduced changes in crystal violet concentration, incubation temperature and washing times, we optimised this important protocol and made it functional for the AGBs. As a result,

we confirmed via crystal violet assay (see M&M section) the initial notion that bacteria growing on the surface of AGBs form more biofilm than their glass bead counterparts (Fig 9.).

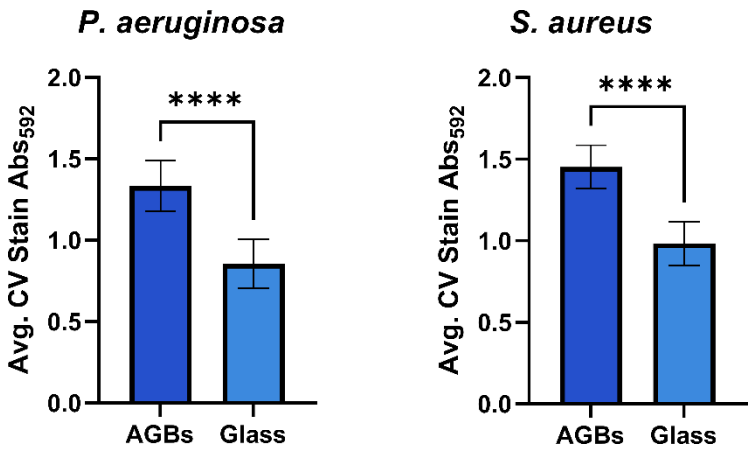

Fig. 9. Comparative biofilm formation of *P. aeruginosa* and *S. aureus* on AGBs vs. glass beads after 48 hours of incubation using the modified crystal violet staining protocol. Bar charts represent the average absorption of the dye at 592nm that remained bound to the biofilms, a qualitative measure of biofilm formation capacity. We measured ten repetitions for each species on each substratum (N=10). The samples were compared via the Wilcoxon-Mann-Whitney test. One asterisk represents $p<0.05$, two asterisks for $p<0.01$, three for $p<0.001$ and four for $p<0.0001$.

Agarose-gelatine beads can serve as small molecule reservoirs. In contrast to other abiotic biofilm substrates, the permeability of crosslinked agarose could serve as a reservoir of small molecules such as nutrients, quorum sensing molecules, drugs, etc. This is an advantage that can be exploited for some experimental setups. Importantly, it is expected that the same scenario could be accounted for *in vivo* biofilms where bacteria are sometimes attached to host surfaces as a mucosal layer and other times on necrotic tissue debris because of bacterial action. The potential implications of this research for *in vivo* biofilms and bacterial action are significant, as this effect is complicated to simulate with other substrates like glass or plastic materials. Our experiments have two bacterial models that produce traceable substances that can potentially accumulate within the beads. We also suggest that this hydrogel could facilitate the diffusion of soluble molecules, including nutrients and bacterial quorum-sensing molecules, while retaining some molecules within its structure as a reservoir, as expected in many *in vivo* systems.

One example is the production of staphyloxanthin, a carotenoid secreted by *S. aureus* that protects *S. aureus* from oxidative stress caused by reactive oxygen species (ROS)[83]. Staphyloxanthin is present in the cell membranes, protecting lipids, proteins and DNA from ROS. The main enzymes against ROS defence are catalases and superoxide dismutase, while the pigment staphyloxanthin is an additional

protection[84]. Clinical samples from diabetic patient foot ulcers showed that staphyloxanthin impairs wound healing *in vivo* and leads to improved survival of *S. aureus* in the presence of free oxidative radicals[85].

In contrast to glass beads, we noticed that the agarose beads were consistently yellower, indicating the pigment's diffusion to the beads' inner part, indicating the accumulation of staphyloxanthin in a similar way as observed for pyoverdine.

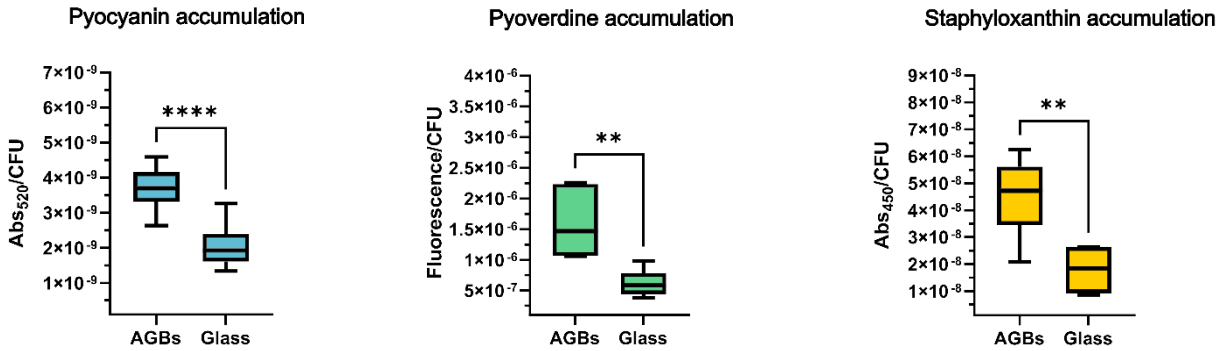

Fig. 10. Comparative amounts of different virulence factors from *P. aeruginosa* and *S. aureus* on agarose-gelatine beads after 48 hours of incubation. Boxplots of pyocyanin and pyoverdine (produced by *P. aeruginosa*) and staphyloxanthin (produced by *S. aureus*) from biofilms after 48 hours of incubation (N=6). The samples were compared via the Wilcoxon-Mann-Whitney test. One asterisk represents $p<0.05$, two asterisks for $p<0.01$, three for $p<0.001$ and four for $p<0.0001$. The Boxes extend from the 25 to the 75 percentiles, and the whiskers represent minimal and maximal values, with the middle line representing the mean.

Discussion

Our biofilm model holds significant potential for a wide range of research applications (see Fig. 11). AGBs can be used to test anti-biofilm molecules, evaluate surface protection compounds, study quorum sensing mechanisms, investigate biofilms on foreign bodies, and conduct microscopy and 'omics profiling studies of biofilms. Additionally, our system is compatible with traditional experimental approaches, including crystal violet quantification and live and scanning electron microscopy.

One of the most exciting applications of our system of agarose-gelatine beads is the ease of conjugating molecules to the surface of the beads. The chemical modification of the AGBs is a great advantage, as we showed in this study with the example of conjugating them with melittin and how the attachment of this antimicrobial and antibiofilm peptide significantly reduced biofilm formation by *E. coli*, *P. aeruginosa*, and *S. aureus*. The idea of using melittin is that honeybee colonies are an

excellent environment for the growth of microorganisms owing to high humidity and temperature, leading honeybees to develop defence mechanisms against this increased risk of pathogen growth[86]. One such defence is a part of their venom, melittin, a small cationic peptide composed of 26 amino acid residues spread on the surfaces of the honeybee nests[87]. As a major constituent of bee venom, melittin forms 50% of the bee venom dry weight[88]. Melittin has been shown to have antibacterial activity against antibiotic-resistant bacteria under both *in vitro* and *in vivo* conditions[89]. It has been reported that honeybees use their venom as a tool of social immunity, trying to protect their colony from pathogen invasion[90]. The bee wax comb acts as the surface where bees deposit melittin, providing collective protection to the colony[91].

The ability to crosslink agarose with various chemical compounds presents a versatile tool for biofilm research, allowing for the exploration of anti-biofilm agents aimed at surface protection, a promising avenue for further research into anti-biofilm compounds and their applications in preventing biofilm-related issues in medical and industrial settings. Explaining this property of easy compound conjugation in the other direction is also possible, such as investigating what elements stimulate biofilm attachment[92]. This knowledge can also be useful to avoid certain materials or to use them in beneficial biofilms where it is convenient to promote the attachment[93].

Agarose-gelatine beads exhibit a unique capability to serve as reservoirs for small molecules, setting them apart from other abiotic biofilm substrates. The permeability of crosslinked agarose allows it to store and gradually release nutrients, quorum-sensing molecules, drugs, and other minor compounds, thus providing a more accurate simulation of *in vivo* biofilm conditions[94]. This feature is particularly advantageous for experimental setups that aim to replicate complex environments where bacteria adhere to host surfaces or necrotic tissue debris. The diffusion of important virulence factors such as staphyloxanthin, pyoverdine, pyocyanin, and quorum-sensing molecules exemplified this capability. It is known that a substantial reduction in staphyloxanthin production tends to occur in correlation with biofilm maturation[95]. In addition, staphyloxanthin accumulation within the AGBs, as we have shown, could be responsible for inhibiting pigment production.

The biofilm system based on AGBs proves effective for detecting genetic factors influencing biofilm formation. This was demonstrated by studying mutant strains deficient in biofilm formation, explicitly focusing on the *fimH* of *E. coli*[96] and the *pfpI* gene in *P. aeruginosa*[97]. The AGBs showed that detecting strains deficient in the biofilm formation of different species is possible. Comparing biofilm formation in AGBs between mutant and wild-type strains revealed a significant reduction in the mutants' biofilm

formation, validating the AGB system's capability to detect variations in biofilm formation under controlled conditions.

Our AGBs serve as a complementary model to biofilm growth studies on glass beads[98]. While glass beads are more suitable for exploring biofilm formation on abiotic surfaces, the AGBs provide a valuable alternative for studying biofilms in environments resembling organic or nutrient-rich conditions. This dual approach enhances our understanding of biofilm dynamics across diverse surfaces. Studies of biofilms using crosslinked AGBs, however, face some limitations. For example, the beads' nutrient composition and diffusion dynamics can differ from those in real-world settings, which may influence biofilm growth patterns and microbial interactions. Therefore, while helpful, these models should be complemented with other systems to obtain a more comprehensive understanding of biofilm biology.

The quantitative proteomic profiling performed in this study revealed distinct protein expression profiles for *E. coli*, *P. aeruginosa*, and *S. aureus* biofilms grown on AGBs compared to glass beads. Some studies suggest that bacterial growth on abiotic surfaces significantly differs from the bacteria from *in vivo* biofilm-related infections[99]. Many of the proteins that were more abundant in AGBs for the two pathogenic bacteria are some crucial virulence factors for *P. aeruginosa* and *S. aureus*, likely reflecting differences in surface sensing due to the chemical composition of the beads.

For *E. coli*, the most differentially upregulated proteins in biofilms on AGBs vs glass beads were ribosomal proteins. This is not a surprising result as this is the most abundant protein group in every cell, so changes to its regulation would amount to significantly differential ribosome stoichiometry[100]. The same trend can be seen in *P. aeruginosa* and *S. aureus*, with around 50 ribosomal structural proteins showing significantly different expression levels. The increased abundance of these ribosomal proteins indicates differences in ribosomal content and activity in biofilms on AGBs.

For *P. aeruginosa*, important virulence factors were more abundant on AGBs than glass beads. Elastase (LasB), the most highly expressed protein, is regulated by the LasR/LasI quorum-sensing system, indicating robust virulence factor activity in biofilms grown on AGBs. Other upregulated virulence factor proteins included the pyoverdine synthesis pathway, which is essential for iron chelation from host cells and plays a role in *in vivo* infections. Conversely, components of the Sec translocon system, such as YajC and SecF, had lower abundance in AGBs, suggesting reduced protein export and altered membrane dynamics compared to glass bead biofilms. The transcription factor

AmrZ (AlgZ) was also downregulated, implying higher levels of alginate, as observed *in vivo P. aeruginosa* biofilms.

Depending on the surface type, *S. aureus* biofilms show significant differences in protein expression and gene regulation responses. Biofilms on AGBs and glass exhibit distinct regulators affecting the transcription of the main *S. aureus* quorum sensing system *agr*. This system produces and senses the autoinducing peptide signal and triggers the response regulator. The genes agrBDCA, organised in the primary transcript RNAII, and the RNAIII transcript downstream drive effects in many virulence genes. Both have close promoters, P2 and P3. A weak promoter, P1, also drives the expression of the response regulator of the agr system, agrA. Although we did not observe changes in the abundance of the *agr* quorum sensing system's components, we identified many regulatory proteins that carefully mediate its expression and downstream effects. Our analysis revealed a significant abundance of CodY and SrrA on AGBs, while SarR is abundant on glass beads. CodY represses the P1 promoter, SarR inhibits P2 expression by inhibiting SarA, and SrrA represses the P2 and P3 promoters. CodY also impacts more than 200 other target genes with similar P1 promoters in the S. aureus genome, mainly via agr. It helps manage signals for nutrient limitation and population size through direct interaction with metabolites and involvement in quorum sensing. On one hand, CodY indicates that most AGB biofilm cells are in a quasi-stationary phase or are part of a mature biofilm. On the other hand, in an *in vivo* context, it functions as a switch that allows the pathogen to limit damage to the host in the long run, reducing the stress of the interaction. SrrA, part of the two-component system SrrAB, senses low oxygen concentration and provides resistance to H2O2 and oxygen radicals by upregulating essential enzymes such as catalase (KatA) and AhpC.

In *S. aureus*, virulence traits are tightly controlled by many regulators that fine-tune gene expression and translation according to environmental signals and surface sensing. We noticed changes in the abundance of components of such systems and numerous regulators, although they were below the threshold of at least 1 log2FC set for this analysis. Nonetheless, these differences drive global changes in the composition of exoenzymes, pathogenicity mechanisms, and cell metabolism. Our results indicate a significant phenotypical effect, substratum and quorum sensing dependent, occurring within the same strain under similar media conditions. *S. aureus* upregulates critical factors enabling intracellular invasion and evasion of the immune system by upregulating Type VII secretion, catalase, and alpha-haemolysin on AGBs. There are abundant fibrinogen-binding proteins on glass beads and several antigens, proteases, phenol-soluble modulin, coagulase, and gamma haemolysin, among others. Biofilms from AGBs and glass appear as two discrete phenotypes: the former represents a

mature and established biofilm, while the latter represents a phenotype closer to a bloodstream infection, where *S. aureus* produces various factors for host cell recognition, utilisation of host resources, attachment, clumping, and virulence factor production. As seen with Staphyloxanthin, whereby biofilms on AGBs shut down their biosynthesis after reaching an optimum in its concentration, we can assume that *S. aureus* also manages and coordinates all other factors according to such optima as the need arises.

It does not escape our attention that this new biofilm model presents a versatile platform with several significant applications. Firstly, it may enable *in vivo* experiments that investigate biofilms in the context of infections associated with foreign objects, providing crucial insights into the dynamics and treatment of such infections. Secondly, the hydrogel material could be potentially used in bioengineering and 3D printing as a biopolymer for fabrication, opening avenues for advanced tissue engineering and regenerative medicine. Lastly, AGBs can serve as an effective model for understanding the role of biofilms in bacterial resistance to antibiotics, allowing the scientific community to conduct experimental evolution studies that could lead to novel strategies for combating antibiotic resistance and biofilm-associated infections. Besides, because of the hydrogel nature of the AGBs, there is also a potential utilisation to study liquid air interface biofilm.

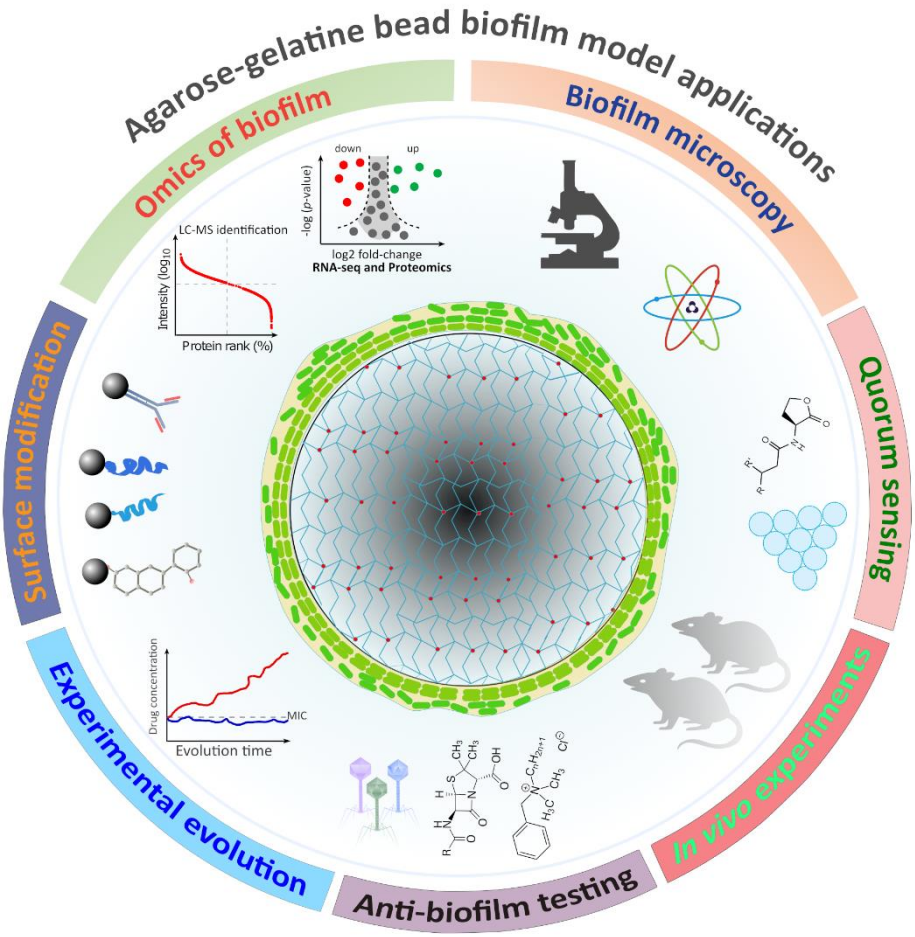

Fig. 11. Summary of the potential applications of the new model of crosslinked agarose-gelatine beads. These beads, with their biocompatibility, ease of preparation, and versatile physical properties, hold significant potential as substrates for biofilm-related research and applications. Their adaptability to mimic various environmental conditions, from nutrient-rich to nutrient-limited, provides a versatile platform for studying biofilms under different scenarios. They can be used to investigate antibiofilm agents, evaluate the efficacy of various compounds in disrupting or inhibiting biofilm formation, and develop new antibacterial treatments and coatings. Moreover, these beads can facilitate studying quorum sensing (QS) mechanisms within biofilms. Furthermore, the beads are compatible with various analytical techniques, including live fluorescence and scanning electron microscopy.

Conclusions

In this study, we have introduced a new substrate based on crosslinked agarose-gelatine hydrogel in the form of beads as a novel strategy to investigate biofilms of bacterial pathogens. The bead method presented here offers the scientific community a new *in vitro* system to investigate bacterial biofilms in a microenvironment resembling that found in biofilm-related infections. We have shown that this method is compatible with various biofilm structural studies and quantitative techniques, including live microscopy techniques such as confocal microscopy and scanning electron microscopy. Our model

is also compatible with other biofilm quantitative techniques, including crystal violet staining and the determination of viable cells, for which we have established adapted protocols to maximise recovery and dispersion of cells using enzymatic and mechanical disruption of the biofilm. Importantly, the agarose-gelatine bead model provides a unique opportunity to study biofilm physiology, as the permeability of the hydrogel beads allows the diffusion of small molecules, including drugs, nutrients, quorum sensing signalling molecules, and other substances in contact with the biofilm or produced by bacterial cells, such as siderophores and other secretion products. We have demonstrated that the beads maintain their properties for an extended period, at least several months, and can preserve biofilm samples using common laboratory anti-freeze agents like DMSO and store them at -80°C indefinitely, providing a reliable long-term preservation option. Furthermore, this system offers additional options that are more challenging with other substrates, such as studying biofilms at an aqueous/air interface since the hydrogel maintains the necessary basal humidity if part of the bead is in contact with the culture medium.

Material and methods

Generation of agarose-gelatine beads. To produce the bead substrate, 4 g of each agarose and gelatine were added to a volume of 200 ml of distilled water in a 400 ml bottle and autoclaved for 20 minutes at 121 °C and 1 atmosphere. After sterilisation and throughout the production process, the liquid mixture was kept liquid by placing the flask on a hot plate of the stirrer at 65 °C with moderate mixing. In a separate container, 500 ml of mineral oil (Merck, Germany) was placed in a cold ice water bath. The oil was previously degasified to remove air bubbles using a vacuum pump. We used two procedures to produce the agarose-gelatine beads. First, we used a multistep pipette (Eppendorf, Germany) to spot around 40 µl of substrate in the cold mineral oil, ensuring that the tip was between 1 to 2 cm from the surface of the oil to avoid deformation of the beads while solidifying or partitioning of the drops (See Fig. S1). A second and higher throughput method incorporated a peristaltic pump P-1 (Pharmacia Biotech, Sweden) that allows a continuous and semiautomatic dropping of the beads into the mineral oil (Fig. 1). At the end of the silicon tubing, a 2 mm internal diameter stainless steel capillary was incorporated for a more precise holding and stable drops, two silicone tubes with a diameter of 3 mm and a length of 0.5 m were extended with one metal tube of the same diameter and a length of 20 cm. The flexible ends were connected to the peristaltic pump, while the ends with the metal tubes opened into the bottle with the substrate or above the collection beaker, respectively. The movement of the peristaltic pump resulted in a stable output of uniform drops of the agarose-gelatine mix, which solidified upon entering the inert, cooled mineral oil, forming ~4 mm Agarose-

gelatine beads (AGBs). After processing, the beads were sieved and washed with distilled water with at least 50 volumes until the oil was totally removed, allowing them to rest for five minutes between washes to allow the oil separation from the aqueous phase.

Crosslinking of the agarose-gelatine beads. The washed and clean agarose beads were crosslinked using divinyl sulfone (DVS) using a modified method from the original described elsewhere[31]. The beads were weighed to calculate the required amount of DVS (v/w%) (Merck, Germany). Approximately 500 ml of 0.5 M sodium carbonate buffer, pH 11.0, was used per 100 grams of gel beads (five volumes). The beads were gently transferred with the help of a funnel to an 800 ml flask, capped, and the crosslinking reaction was initiated by adding DVS, a final concentration of 0.5%. The reaction was allowed to proceed on a shaker at room temperature overnight, covering the beaker with parafilm to prevent evaporation. The next day, the beads were thoroughly washed with distilled water by decanting and sieving until a neutral pH was achieved. To remove residual amounts of unreacted vinyl groups, we placed the beads in five volumes of 0.5 M sodium carbonate buffer, pH 9, and β-mercaptoethanol was added for a final concentration of 0.5%. The flask was incubated with shaking overnight in the dark at room temperature. Afterwards, 500 ml of distilled water was used to wash the beads five times. To remove fully the unreacted vinyl group, the beads were covered with five volumes of 1 M sodium carbonate, pH 10, and glycine was added for a final concentration of 10% (w/v). The reaction was also conducted overnight at room temperature with shaking. The next day, the beads were washed three times with five volumes of 0.1 M carbonate-bicarbonate buffer at pH 10 and a 0.1 M citrate buffer at pH 4.0. The beads were rewashed with five volumes of distilled water three times and added directly to a flask containing five volumes of bacterial culture media LB or Mueller-Hinton broth (MHB). The bottles were autoclaved and stored at +4 °C until use. For a step-by-step protocol, see Protocol I of supplementary materials.

844 **Bacterial strains and cultivation conditions.** *Escherichia coli* K-12 MG1655[101], *Escherichia coli*
845 BW25113, and its derivative mutant *Escherichia coli* BW25113 *fimH::*Kn, both from the Keio
846 collection[102], *Pseudomonas aeruginosa* PAO1[103], *Pseudomonas aeruginosa PA14* [104] *and its derivative*
847 *mutant Pseudomonas aeruginosa PA14 pfpI::*MAR2xT7[104], and *Staphylococcus aureus* SH1000[105] were
848 the strains used for different experiments across this study. Generally, bacteria were cultivated on
849 Petri dishes from frozen glycerol stocks on lysogeny broth (LB) agar and incubated overnight at 37 °C.
850 The next day, a single colony was inoculated into 10 ml of liquid LB in 50 ml Falcon tubes and shaken
851 at 200 rpm overnight at 37 °C. The total cell density was determined by measuring the optical density
852 (OD) in a spectrophotometer at 600 nm. The inoculums were diluted to approximately 10^6 CFU/ml per
853 culture for biofilm inoculation.
854
855 **Biofilm cultivation.** For biofilm culturing, two beads were aseptically transferred to each well of a non-
856 binding polypropylene 24-well microplate (Carl Roth, Germany). Overnight cultures of *Pseudomonas*
857 *aeruginosa, Staphylococcus aureus* SH1000, and *Escherichia coli* K-12 MG1655 in LB medium were
858 diluted to an optical density of approximately $1x10^5$ CFU/ml and added to the microplate containing
859 the beads (1 ml per well). The 24-well microplate was then placed in a multiwell plate shaker with
860 moderate shaking (20-30 rpm) at 37 °C for 24 and 48 hours. After 24 hours of incubation, the beads
861 were gently washed with sterile 0.9 % NaCl saline solution by pipetting, and a fresh medium was
862 added.
863

Biofilm viable bacterial enumeration. After biofilm cultivation, each bead was transferred with sterilised tweezers into a 1.5 ml microcentrifuge tube (Safe-Lock Tubes, Eppendorf) containing 1 ml saline. The samples were sonicated in an ultrasonic bath to detach the biofilm from the bead surface and separate the bacteria at 40 kHz for 3 min[98]. Before and after sonicating, each microcentrifuge tube contained a bead and a vortex vigorously mixed with the saline solution. The tubes were centrifuged at 10,000 x g for 3 minutes, and the pellets resuspended in 200 µl of digestion buffer (150 mM NaCl, 50 mM Tris-buffer, 10 mM $MgCl_2$, 5 mM L-cysteine, 5 mg/ml DNAse I, 2 mg/ml RNAse A, pH 7.5) and incubated at 37°C for 15 minutes. Afterwards, 20 µl of papain stock solution (10 mg/ml) was added to each tube and incubated for another 15 minutes at 37°C in moderate shaking. The tubes were centrifuged at 10,000 x g for 3 minutes and resuspended in 1 ml of 0.9% NaCl. A volume of 20 µl of each sample was transferred to the wells of the first row of a 96-well microplate. Using a multichannel pipette, all samples were diluted in 1:10 steps (20 µl sample; 180 µl saline) from the first row to the last. Droplets of 10 µl for each dilution were spotted on pre-dried LB agar plates (for 45 minutes before use in a laminar flow cabinet). The wells containing the bacterial dilution were carefully mixed by pipetting before spotting the drops. After drying the droplets (approximately 5–10 minutes), plates were incubated for 16 hours at 30°C. The next day, the microcolonies were observed and, if necessary, allowed to grow for another two hours at 37°C. Then, the colonies were counted for the first dilution, which resulted in a countable range of 5–35 colonies; the bacterial number was determined, keeping into account the dilution factor, and expressed in CFU/ml.

GFP-tagging. To perform live fluorescent microscopy of bacterial biofilms on the surface of agarose-gelatin beads, a constitutive green fluorescent protein (GFP) gene was inserted into the chromosome of *E. coli* MG1655 following the methodology described elsewhere[106]. Briefly, the *E. coli* DH5α carrying the kanamycin resistance plasmid pGRG36-Kn-PA1-GFP was used as a plasmid donor to integrate a GFP expression cassette into the chromosome of *E. coli* MG1655. The plasmid pGRG36-Kn-PA1-GFP was purified using the Pure Yield Plasmid Miniprep System (Promega, USA) following the manufacturer's instructions. The purified plasmid was stored at -20 °C until use. A mid-exponential culture (100 ml) of *E. coli* MG1655 was grown until an OD_{600} between 0.4 and 0.6 was reached. The cells were made competent using the previously described protocols for chemical transformation[107] and they were transformed with the pGRG36-Kn-PA1-GFP plasmid. The phenotype of kanamycin resistance and green fluorescence were checked, and positive clones were selected.

Crystal violet staining. Qualitative quantitation of all biofilm components was performed using crystal violet staining (O'Toole 2011). For the substrate comparison, AGBs (4 mm) and glass beads (4 mm, Merck) were inoculated with *Pseudomonas aeruginosa* PAO1 and *Staphylococcus aureus* SH1000.

After the maturation of the biofilm in 24-well polypropylene plates (Carl Roth, Germany) and a final wash, the beads in each well were covered with 500 µl of NaCl 0.9% saline solution and another 500 µl of a 0.1 % crystal violet (Sigma-Aldrich) in saline for 1 min. Using a single-channel pipette, the staining solution was aspirated and discarded. The beads were carefully rinsed by adding 1 ml of distilled water several times. The washing process was repeated until the water was clear or the wash had an OD592 below 0.01. To solubilise crystal violet retained by the biofilm, 1 ml of a mixed solution of 95 % Ethanol[108] and 0.05% of Triton X-100 [109] were added to each well. The beads were incubated on a shaker at room temperature for 30 minutes at 45 °C. 200 µL of each sample were then transferred to the wells of a 96-well plate. The amount of crystal violet was estimated by absorbance at 592 nm.

Scanning electron microscopy. To visualise biofilm formation on the surface of the bead substrate, images of colonised Agarose-gelatine beads were taken using a scanning electron microscope (SEM) (EVO MA 10, Zeiss). Before removal from the 24-well plates where the biofilm developed, the samples were washed with saline, as described above. The following fixation steps were carried out under the safety cabinet due to the high toxicity of the chemicals used. Six samples of mature biofilm produced by *Pseudomonas aeruginosa* PAO1 and *Staphylococcus aureus* SH1000, grown on AGBs, were collected in a 10 ml glass jar using sterile forceps. Fixation was performed by covering the samples with 5 ml of 2.5 % glutaraldehyde (glutaraldehyde 25 %, Roth) in 0.05 M Cacodylate buffer for 1 hour (Jacques and Graham 1989). Glutaraldehyde creates irreversible cross-linking networks throughout the cytoplasm and is suitable for preserving cellular ultrastructure. Once the samples are in the fixing solution, they can be stored at -4 °C for several weeks. The fixing solution was stepwise substituted by 0.05 M Cacodylate buffer for further preparation, ensuring the beads never dried completely. The samples were then rinsed three times with 0.05 M Cacodylate buffer, each lasting 10 minutes. Osmium tetroxide, whose primary purpose is contrasting, was used as a secondary fixation agent[110]. Two millilitres of 2 % Osmium tetroxide (ReagentPlus®, 99.8%, Sigma-Aldrich) in distilled water were added to the samples immediately after removal of the buffer and incubated for an additional 30 minutes. Another washing with Cacodylate buffer followed as previously described. Dehydration of the fixed colonised AGBs was performed using alcohol of different concentrations. This was done in preparation for the critical point drying with Carbon dioxide (CO_2). The samples were transferred directly into the critical point dryer's magazine (Foissner vessel) (CPD 030, BAL-TEC) for better handling. The alcohol series consisted of 30%, 50%, 70%, 90%, 2x 100%, and 2x 100% alcohol with a molecular sieve. Starting with the lowest concentration, the Foissner vessel was placed in a beaker filled with alcohol and incubated for 10 minutes. The dehydration process was continued sequentially, using the highest

alcohol concentration, including a molecular sieve. The Foissner vessel with the samples was now placed in the cabin of the critical point dryer, and the remaining water and alcohol were entirely replaced by liquid CO_2. Liquid CO_2 changes into the gaseous phase at 31 °C and 74 bar. In this way, the surface structure of a sample can be preserved, which would be damaged in the presence of water during the transition from the liquid to the gaseous state. After drying, the samples were mounted on 12 mm aluminium stubs and coated with gold using a sputtering system (SCD 040, BALZERS). The SEM works with electrons; only conductive surfaces can be examined. For an even gold layer on the preparations, the air in the coater was replaced by inert Argon. The samples were then placed in the SEM and recorded at working distances (WD) from 6.5 mm to 12 mm and magnifications between 50 and 27 k times.

Confocal fluorescence microscopy. The advantage of imaging with a confocal fluorescence microscope in biofilms is that the cells remain viable. The extracellular polymeric substance (EPS) is preserved; thus, the biofilm remains intact. This way, the bead surface cell density can be determined more precisely. The Agarose-gelatine beads were cultivated with *Escherichia coli* K-12 MG1655-GFP, as described before. After maturation and a last washing step with saline, the samples were transferred into a chambered coverslip with 8 wells and a glass bottom for high-end microscopy (µ-Slide 8 Well, Ibidi, Germany). The beads in the chambers were covered with saline, the coverslip was closed with a lid, and the images were acquired with an inverted confocal laser scanning microscope (SP8-1, Leica) equipped with a 40x/1.25-0.75 objective. GFP was excited from 488 nm and detected at 510 nm. Both single images and Z-stacks were created from the bead surface or cross sections and later edited in Image J.

Coupling of melittin to the agarose-gelatine beads. We modified the method described in Steven C. March *et al* [111] to couple melittin with the agarose beads using affinity chromatography principles. The washed agarose beads, as described in a previous section of this manuscript, were first activated with cyanogen bromide (CNBr). A volume of 500 µl of coupling buffer (0.1 M Sodium bicarbonate, pH 9.5 in distilled water) along with the amino ligand to be coupled, in our case melittin (5 mg/ml, Genescript, USA) and Bovine serum albumin (BSA) (1 mg/ml, Merck) was used per bead. The coupling reaction was carried out for 20 hours at 4°C. After the coupling reaction, the beads were washed with 20 volumes of buffer containing 0.1 M sodium acetate, pH 4, 2 M urea and 0.1 M sodium bicarbonate, pH 10. The beads were then dialysed against 100 volumes of NaCl 9% and stored at 4°C. All operations were made under sterile conditions under a laminar flow with filtered sterilised buffer to prevent bead contamination.

966 **Quantification of the virulence factor Pyocyanin.** To investigate substrate-dependent virulence, from
967 all wells of the 24-well plate containing *Pseudomonas aeruginosa* PAO1 samples, the bacterial
968 supernatant from 6 biofilm-containing samples on glass or AGBs was collected and transferred into 15
969 ml Falcon tubes. The samples were centrifuged at 4,000 rpm for 15 minutes at 20°C. The resulting
970 supernatant was then separated from the bacterial pellets and used for further purification and
971 quantification of Pyocyanin concentration. Pyocyanin was extracted as described previously[112] with
972 modifications. Briefly, 5 ml of the supernatant obtained from each sample was incubated with 1 ml
973 chloroform for 10 minutes, with twice vortexing in between. The reaction settled an organic phase
974 (blue colour) at the bottom of the tubes, from which 900 µl were pipetted out and transferred into 1.5
975 ml microcentrifuge tubes. The samples were centrifuged for 1 minute at 10,000 rpm to remove
976 impurities. 700 µL of the organic phase was transferred to a new microcentrifuge tube and further
977 extracted with 700 µl 0.1N HCl solution. From each sample, 7x100 µl of the aqueous phase formed at
978 the top (red colour) was transferred to a 96-well plate, and the absorbance was measured at 520 nm
979 using a spectrophotometer with the 0.1N HCl solution used as a blank.
980
981 **Staphyloxanthin accumulation.** *S. aureus* SH1000 biofilms growing in AGBs or glass beads were grown
982 in 2 ml of M9 medium with moderate shaking at 37°C for 48 hours with a medium change at 24 hours.
983 The M9 medium (Merck, Germany) used for this experiment was supplemented with 0.4% casamino
984 acids (Carl Roth, Germany), 5 mM MgSO4 (Carl Roth, Germany), and 0.5% glucose as carbon sources
985 (final concentrations). Glucose and magnesium salt were added after autoclaving. Cultures were
986 centrifuged for 1 minute at 10,000 x g, and the supernatant was removed. Each bead was washed
987 twice with 1 ml of NaCl 0.9% solution and added 500 µL of methanol and incubated at 55°C for 30
988 minutes. Tubes were centrifuged for 2 minutes at 10,000 x g. 300 µL from each tube was added to
989 each well of a polystyrene 96-well plate and then quantified at OD_{450} nm on a GloMax Explorer plate
990 reader (Promega, USA). Five biological replicates were performed for each group. For normalisation,
991 all OD_{450} values were divided by the CFU count of each bead. Normalised production of
992 staphyloxanthin was expressed as a ratio of OD450/CFU and compared.
993
994 **Agarose-gelatine stiffness measurement**. The stiffness of agarose-gelatine beads, both with and
995 without crosslinking, was measured using a static compression test described elsewhere[113]. The beads
996 (4 mm) were directly used for the measurement. Then, beads were placed at room temperature
997 overnight for temperature equilibration before the mechanical testing. Young's modulus was
998 determined by fitting a line to the linear region of the stress-strain curve. Five samples were used for
999 each measurement.

1000 **Sample preparation for proteomics of bacterial biofilms.** Each experimental condition consisted of
1001 six replicates. A volume of 500 µl of denaturation buffer (6M urea/2 M thiourea in 10 mM HEPES pH
1002 8.0) was added into each sample consisting of three beads of glass, agarose-gelatine and polystyrene
1003 substrate from multiwell plates. The samples went for five freeze-thaw cycles to cause lysis and
1004 protein release. The resulting lysate was used for in-solution protein digestion as described previously
1005 [114]. Briefly, proteins, re-suspended in denaturation buffer, were reduced by the addition of 1 µl of 10
1006 mM DTT dissolved in 50 mM ammonium bicarbonate (ABC) and incubated for 30 minutes, followed
1007 by a 20-minute alkylation reaction with 1 µl of 55 mM iodoacetamide. As a first digestion step, Lysyl
1008 endopeptidase (LysC, Wako, Japan) resuspended in 50 mM ABC was added to each tube in a ratio of
1009 1 µg per 50 µg of total proteins and incubated for 3 hours. After pre-digestion with LysC, protein
1010 samples were diluted four times with 50 mM ABC and subjected to overnight trypsin digestion using
1011 1 µg/reaction of sequencing grade modified trypsin (Promega, USA), also diluted before use in 50 mM
1012 ABC. All in-solution protein digestion steps were performed at room temperature. After adding
1013 iodoacetamide, the samples were protected from the light until the digestion was stopped by
1014 acidification, adding 5% acetonitrile and 0.3% trifluoroacetic acid (final concentrations). The samples
1015 were micro-purified and concentrated using the Stage-tip protocol[114] and the eluates were vacuum-
1016 dried. For a step-by-step protocol, see Protocol IV of supplementary materials.

1017

1018 **Nano liquid chromatography-mass spectrometry (LC-MS) and data analysis.** Peptides were
1019 reconstituted in 30 µl of 0.05% trifluoroacetic acid, 4% acetonitrile in water, and 2 µl were analysed
1020 by an Ultimate 3000 reversed-phase capillary nano liquid chromatography system connected to a Q
1021 Exactive HF mass spectrometer (Thermo Fisher Scientific). Samples were injected and concentrated
1022 on a trap column (PepMap100 C18, 3 µm, 100 Å, 75 µm i.d. x 2 cm, Thermo Fisher Scientific)
1023 equilibrated with 0.05% TFA in water. After switching the trap column inline, LC separations were
1024 performed on a capillary column (Acclaim PepMap100 C18, 2 µm, 100 Å, 75 µm i.d. x 25 cm, Thermo
1025 Fisher Scientific) at an eluent flow rate of 300 nl/min. Mobile phase A contained 0.1 % formic acid in
1026 water, and mobile phase B contained 0.1% formic acid in 80 % acetonitrile / 20% water. The column
1027 was pre-equilibrated with 5% mobile phase B followed by an increase of 5 - 44% mobile phase B in 35
1028 min. Mass spectra were acquired in a data-dependent mode utilising a single MS survey scan (m/z
1029 300–1650) with a resolution of 60,000 and MS/MS scans of the 15 most intense precursor ions with a
1030 resolution of 15,000. The dynamic exclusion time was set to 20 seconds, and automatic gain control
1031 was set to $3x10^6$ and $1x10^5$ for MS and MS/MS scans, respectively.
1032 MS and MS/MS raw data were analysed using the MaxQuant software package (version 2.0.3.0) with
1033 the implemented Andromeda peptide search engine[115]. Data were searched against the reference

protein sequence databases downloaded from UniProt: *E. coli* (4448 proteins, Proteome ID UP000000625), *P. aeruginosa* (5564 proteins, Proteome ID UP000002438), and *S. aureus* (2889 proteins, Proteome ID UP000008816). Filtering and statistical analysis were performed using the software Perseus version 1.6.14[116]. Missing values are imputed using the default settings. Mean log2 fold protein LFQ intensity differences between experimental groups (glass beads vs. AGBs) were calculated in Perseus using student's t-tests, and *p*-values were adjusted via false discovery rate (FDR) of 0.05 as a cut-off.

Statistical analysis. The student's t-test was used for pair comparisons if sample data followed a normal distribution and had homogenous variance. Otherwise, the Mann-Whitney U-test was used instead. For multiple comparisons, we used one-way ANOVA with the Holm-Šídák test for parametric data or the Kruskal-Wallis test for non-parametric ones. All statistical tests were carried out in GraphPad (Prism, version 9) or R[117].

Acknowledgements. We want to thank the assistance of the Core Facility BioSupraMol (Freie Universität Berlin), which was supported by the Deutsche Forschungsgemeinschaft (DFG).

Funding. This research was part of a multi-institutional project funded by the Volkswagen Stiftung for DR. We also thank the OneHealth PhD program funded by Vetmeduni, WWTF Vienna to ARR, the program Erasmus-Mundus-Master to NP.

Author Contribution. The authors confirm their contribution to the paper as follows: study conception and design: DR and ARR. Data collection and analysis: MH, DR, AN, BK, NP, ARR. Analysis and interpretation of results: MH, DR, AN, BK, NP, JR and ARR. Draft manuscript preparation: DR, MH, AN, ARR. Manuscript editing and correction: all authors. Supervision: JR and ARR. Funding and resources: JR and ARR. All authors reviewed the results and approved the final version of the manuscript.

References

1. Stoodley, P., Sauer, K., Davies, D. G. & Costerton, J. W. Biofilms as complex differentiated communities. *Annu Rev Microbiol* **56**, 187–209 (2002).
2. Römling, U. Is biofilm formation intrinsic to the origin of life? *Environ Microbiol* **25**, 26–39 (2023).
3. Hall-Stoodley, L., Costerton, J. W. & Stoodley, P. Bacterial biofilms: from the Natural environment to infectious diseases. *Nature Reviews Microbiology 2004 2:2* **2**, 95–108 (2004).
4. Bar-On, Y. M. & Milo, R. Towards a quantitative view of the global ubiquity of biofilms. *Nature Reviews Microbiology 2019 17:4* **17**, 199–200 (2019).
5. Flemming, H.-C. & Wuertz, S. Bacteria and archaea on Earth and their abundance in biofilms. *Nat Rev Microbiol* **17**, 247–260 (2019).

6. Cunliffe, M. & Murrell, J. C. The sea-surface microlayer is a gelatinous biofilm. *The ISME Journal 2009 3:9* **3**, 1001–1003 (2009).
7. Bjarnsholt, T. The role of bacterial biofilms in chronic infections. *APMIS Suppl* 1–51 (2013) doi:10.1111/apm.12099.
8. Trubenová, B., Roizman, D., Moter, A., Rolff, J. & Regoes, R. R. Population genetics, biofilm recalcitrance, and antibiotic resistance evolution. *Trends Microbiol* **30**, (2022).
9. Del Pozo, J. L. Biofilm-related disease. *Expert Rev Anti Infect Ther* **16**, 51–65 (2018).
10. Seneviratne, C. J., Zhang, C. F. & Samaranayake, L. P. Dental plaque biofilm in oral health and disease. *Chin J Dent Res* **14**, 87–94 (2011).
11. Vestby, L. K., Grønseth, T., Simm, R. & Nesse, L. L. Bacterial Biofilm and its Role in the Pathogenesis of Disease. *Antibiotics 2020, Vol. 9, Page 59* **9**, 59 (2020).
12. Høiby, N. *et al.* The clinical impact of bacterial biofilms. *International Journal of Oral Science 2011 3:2* **3**, 55–65 (2011).
13. Coenye, T. Biofilm antimicrobial susceptibility testing: where are we and where could we be going? *Clin Microbiol Rev* **36**, (2023).
14. Trubenová, B., Roizman, D., Moter, A., Rolff, J. & Regoes, R. R. Population genetics, biofilm recalcitrance, and antibiotic resistance evolution. *Trends Microbiol* **30**, (2022).
15. Høiby, N. *et al.* ESCMID guideline for the diagnosis and treatment of biofilm infections 2014. *Clin Microbiol Infect* **21 Suppl 1**, S1-25 (2015).
16. Azeredo, J. *et al.* Critical review on biofilm methods. *https://doi.org/10.1080/1040841X.2016.1208146* **43**, 313–351 (2016).
17. Fletcher, M. The effects of culture concentration and age, time, and temperature on bacterial attachment to polystyrene. *https://doi.org/10.1139/m77-001* **23**, 1–6 (2011).
18. Kharazmi, A., Giwercman, B. & Høiby, N. Robbins device in biofilm research. *Methods Enzymol* **310**, 207–15 (1999).
19. Azeredo, J. *et al.* Critical review on biofilm methods. *https://doi.org/10.1080/1040841X.2016.1208146* **43**, 313–351 (2016).
20. Tolker-Nielsen, T. & Sternberg, C. Methods for studying biofilm formation: flow cells and confocal laser scanning microscopy. *Methods Mol Biol* **1149**, 615–29 (2014).
21. Gomes, I. B. *et al.* Standardized reactors for the study of medical biofilms: a review of the principles and latest modifications. *https://doi.org/10.1080/07388551.2017.1380601* **38**, 657–670 (2017).
22. Kher, L., Kelley, K. & Santoro, D. Ultrastructural Analysis of Differences in the Growth and Maturation of Staphylococcus pseudintermedius Biofilm on Biotic and Abiotic Surfaces. *Microbiol Spectr* **11**, e0357722 (2023).
23. Vyas, H. K. N., Xia, B. & Mai-Prochnow, A. Clinically relevant in vitro biofilm models: A need to mimic and recapitulate the host environment. *Biofilm* **4**, 100069 (2022).
24. Bonnet, M., Lagier, J. C., Raoult, D. & Khelaifia, S. Bacterial culture through selective and non-selective conditions: the evolution of culture media in clinical microbiology. *New Microbes New Infect* **34**, 100622 (2020).
25. Austin, B. The value of cultures to modern microbiology. *Antonie Van Leeuwenhoek* **110**, 1247–1256 (2017).
26. Das, N. *et al.* Progress in the development of gelling agents for improved culturability of microorganisms. *Front Microbiol* **6**, 698 (2015).
27. Koch, R. Über den augenblicklichen Stand der bacteriologischen Choleradiagnose. *Deutsche Medizinische Wochenschrift* **19**, 523–525 (1893).
28. World Health Organization. *WHO Bacterial Priority Pathogens List, 2024: Bacterial Pathogens of Public Health Importance to Guide Research, Development and Strategies to Prevent and Control Antimicrobial Resistance*. https://www.who.int/publications/i/item/9789240093461 (2024).

29. EUCAST. The European Committee on Antimicrobial Susceptibility Testing. *Breakpoint tables for interpretation of MICs and zone diameters, Version 14.0* https://www.eucast.org/clinical_breakpoints (2024).
30. Hjertén, S. The preparation of agarose spheres for chromatography of molecules and particles. *Biochimica et Biophysica Acta (BBA) - Specialized Section on Biophysical Subjects* **79**, 393–398 (1964).
31. Porath, J., Låås, T. & Janson, J. C. Agar derivatives for chromatography, electrophoresis and gel-bound enzymes. III. Rigid agarose gels cross-linked with divinyl sulphone (dvs). *J Chromatogr* **103**, 49–62 (1975).
32. Cash, H. A., Woods, D. E., McCullough, B., Johanson, W. G. & Bass, J. A. A rat model of chronic respiratory infection with Pseudomonas aeruginosa. *Am Rev Respir Dis* **119**, 453–459 (1979).
33. Facchini, M., De Fino, I., Riva, C. & Bragonzi, A. Long term chronic Pseudomonas aeruginosa airway infection in mice. *J Vis Exp* (2014) doi:10.3791/51019.
34. Rodríguez-Rojas, A. *et al.* Assessing the emergence of resistance: the absence of biological cost in vivo may compromise fosfomycin treatments for P. aeruginosa infections. *PLoS One* **5**, e10193 (2010).
35. Konrat, K. *et al.* The Bead Assay for Biofilms: A Quick, Easy and Robust Method for Testing Disinfectants. *PLoS One* **11**, (2016).
36. Roizman, D., Vidaillac, C., Givskov, M. & Yang, L. In Vitro Evaluation of Biofilm Dispersal as a Therapeutic Strategy To Restore Antimicrobial Efficacy. *Antimicrob Agents Chemother* **61**, (2017).
37. Er, B., Demirhan, B., Onurdağ, F. K., Özgacar, S. Ö. & Öktem, A. B. Antimicrobial and antibiofilm effects of selected food preservatives against Salmonella spp. isolated from chicken samples. *Poult Sci* **93**, 695–701 (2014).
38. Heukelekian, H. & Heller, A. Relation between Food Concentration and Surface for Bacterial Growth. *J Bacteriol* **40**, 547 (1940).
39. Zobell, C. E. The Effect of Solid Surfaces upon Bacterial Activity. *J Bacteriol* **46**, 39 (1943).
40. Konrat, K. *et al.* The Bead Assay for Biofilms: A Quick, Easy and Robust Method for Testing Disinfectants. *PLoS One* **11**, (2016).
41. Miller, W. R. & Arias, C. A. ESKAPE pathogens: antimicrobial resistance, epidemiology, clinical impact and therapeutics. *Nat Rev Microbiol* (2024) doi:10.1038/s41579-024-01054-w.
42. Murray, C. J. *et al.* Global burden of bacterial antimicrobial resistance in 2019: a systematic analysis. *The Lancet* **0**, (2022).
43. Browning, D. F., Hobman, J. L. & Busby, S. J. W. Laboratory strains of Escherichia coli K-12: things are seldom what they seem. *Microb Genom* **9**, (2023).
44. Mackie, A. *et al.* Addition of Escherichia coli K-12 growth observation and gene essentiality data to the EcoCyc database. *J Bacteriol* **196**, 982–8 (2014).
45. Richter, A. M. *et al.* Evaluation of Biofilm Cultivation Models for Efficacy Testing of Disinfectants against Salmonella Typhimurium Biofilms. *Microorganisms* **11**, (2023).
46. Rodríguez-Rojas, A. *et al.* Antimicrobial Peptide Induced-Stress Renders Staphylococcus aureus Susceptible to Toxic Nucleoside Analogs. *Front Immunol* **11**, 1686 (2020).
47. Rodríguez-Rojas, A. *et al.* Non-lethal exposure to H2O2 boosts bacterial survival and evolvability against oxidative stress. *PLoS Genet* **16**, e1008649 (2020).
48. Prossliner, T., Skovbo Winther, K., Sørensen, M. A. & Gerdes, K. Ribosome Hibernation. *Annu Rev Genet* **52**, 321–348 (2018).
49. Kimura, S. & Suzuki, T. Fine-tuning of the ribosomal decoding center by conserved methyl-modifications in the Escherichia coli 16S rRNA. *Nucleic Acids Res* **38**, 1341–52 (2010).
50. Brandi, A. *et al.* Transcriptional and post-transcriptional events trigger de novo infB expression in cold stressed Escherichia coli. *Nucleic Acids Res* **47**, 4638–4651 (2019).
51. Krupka, M., Sobrinos-Sanguino, M., Jiménez, M., Rivas, G. & Margolin, W. Escherichia coli ZipA Organizes FtsZ Polymers into Dynamic Ring-Like Protofilament Structures. *mBio* **9**, (2018).

1175 52. Rust, L., Pesci, E. C. & Iglewski, B. H. Analysis of the Pseudomonas aeruginosa elastase (lasB)
1176 regulatory region. *J Bacteriol* **178**, 1134–1140 (1996).
1177 53. González-Alsina, A., Mateu-Borrás, M., Doménech-Sánchez, A. & Albertí, S. Pseudomonas
1178 aeruginosa and the Complement System: A Review of the Evasion Strategies. *Microorganisms*
1179 **11**, (2023).
1180 54. Dell'Anno, F. *et al.* Novel Insights on Pyoverdine: From Biosynthesis to Biotechnological
1181 Application. *Int J Mol Sci* **23**, (2022).
1182 55. Ramsey, D. M., Baynham, P. J. & Wozniak, D. J. Binding of Pseudomonas aeruginosa AlgZ to
1183 sites upstream of the algZ promoter leads to repression of transcription. *J Bacteriol* **187**, 4430–
1184 4443 (2005).
1185 56. Kalia, M., Resch, M. D., Cherny, K. E. & Sauer, K. The Alginate and Motility Regulator AmrZ is
1186 Essential for the Regulation of the Dispersion Response by Pseudomonas aeruginosa Biofilms.
1187 *mSphere* **7**, e0050522 (2022).
1188 57. Jones, C. J., Ryder, C. R., Mann, E. E. & Wozniak, D. J. AmrZ Modulates Pseudomonas aeruginosa
1189 Biofilm Architecture by Directly Repressing Transcription of the psl Operon. *J Bacteriol* **195**,
1190 1637 (2013).
1191 58. L, T. & I, C. Pushing the Envelope: The Mysterious Journey Through the Bacterial Secretory
1192 Machinery, and Beyond. *Front Microbiol* **12**, (2021).
1193 59. Fortuna, A., Bähre, H., Visca, P., Rampioni, G. & Leoni, L. The two Pseudomonas aeruginosa
1194 DksA stringent response proteins are largely interchangeable at the whole transcriptome level
1195 and in the control of virulence-related traits. *Environ Microbiol* **23**, 5487–5504 (2021).
1196 60. Lomax, M. S. & Greenberg, G. R. Characteristics of the deo operon: role in thymine utilization
1197 and sensitivity to deoxyribonucleosides. *J Bacteriol* **96**, 501–14 (1968).
1198 61. Sanchez-Herrero, J. F., Bernabeu, M., Prieto, A., Hüttener, M. & Juárez, A. Gene Duplications in
1199 the Genomes of Staphylococci and Enterococci. *Front Mol Biosci* **7**, 160 (2020).
1200 62. Baum, K. R., Ahmad, Z. & Singh, V. K. Regulation of Expression of Oxacillin-Inducible Methionine
1201 Sulfoxide Reductases in Staphylococcus aureus. *Int J Microbiol* **2015**, (2015).
1202 63. Koprivnjak, T. *et al.* Cation-induced transcriptional regulation of the dlt operon of
1203 Staphylococcus aureus. *J Bacteriol* **188**, 3622–30 (2006).
1204 64. Nagel, A. *et al.* Inhibition of Rho Activity Increases Expression of SaeRS-Dependent Virulence
1205 Factor Genes in Staphylococcus aureus, Showing a Link between Transcription Termination,
1206 Antibiotic Action, and Virulence. *mBio* **9**, (2018).
1207 65. Jenul, C. & Horswill, A. R. Regulation of Staphylococcus aureus Virulence. *Microbiol Spectr* **7**,
1208 (2019).
1209 66. Albanesi, D. & de Mendoza, D. FapR: From Control of Membrane Lipid Homeostasis to a
1210 Biotechnological Tool. *Front Mol Biosci* **3**, 64 (2016).
1211 67. Ravcheev, D. A. *et al.* Transcriptional regulation of central carbon and energy metabolism in
1212 bacteria by redox-responsive repressor Rex. *J Bacteriol* **194**, 1145–57 (2012).
1213 68. Kiran, K. & Patil, K. N. Characterization of Staphylococcus aureus RecX protein: Molecular
1214 insights into negative regulation of RecA protein and implications in HR processes. *J Biochem*
1215 **174**, 227–237 (2023).
1216 69. Hübscher, J. *et al.* MsrR contributes to cell surface characteristics and virulence in
1217 Staphylococcus aureus. *FEMS Microbiol Lett* **295**, 251–60 (2009).
1218 70. Pamp, S. J., Frees, D., Engelmann, S., Hecker, M. & Ingmer, H. Spx is a global effector impacting
1219 stress tolerance and biofilm formation in Staphylococcus aureus. *J Bacteriol* **188**, 4861–70
1220 (2006).
1221 71. Makhlin, J. *et al.* Staphylococcus aureus ArcR controls expression of the arginine deiminase
1222 operon. *J Bacteriol* **189**, 5976–86 (2007).
1223 72. Yang, X. *et al.* First-In-Class Inhibitor of Ribosomal RNA Synthesis with Antimicrobial Activity
1224 against Staphylococcus aureus. *Biochemistry* **56**, 5049–5052 (2017).

1225 73. Roux, A., Todd, D. A., Velázquez, J. V, Cech, N. B. & Sonenshein, A. L. CodY-mediated regulation
1226 of the Staphylococcus aureus Agr system integrates nutritional and population density signals.
1227 *J Bacteriol* **196**, 1184–96 (2014).
1228 74. Miyazaki, E., Chen, J. M., Ko, C. & Bishai, W. R. The Staphylococcus aureus rsbW (orf159) gene
1229 encodes an anti-sigma factor of SigB. *J Bacteriol* **181**, 2846–51 (1999).
1230 75. Tajbakhsh, G. & Golemi-Kotra, D. The dimerization interface in VraR is essential for induction
1231 of the cell wall stress response in Staphylococcus aureus: a potential druggable target. *BMC*
1232 *Microbiol* **19**, 153 (2019).
1233 76. Haag, A. F. & Bagnoli, F. The Role of Two-Component Signal Transduction Systems in
1234 Staphylococcus aureus Virulence Regulation. *Curr Top Microbiol Immunol* **409**, 145–198 (2017).
1235 77. Hardie, K. R. & Heurlier, K. Establishing bacterial communities by 'word of mouth': LuxS and
1236 autoinducer 2 in biofilm development. *Nat Rev Microbiol* **6**, 635–43 (2008).
1237 78. Burts, M. L., Williams, W. A., DeBord, K. & Missiakas, D. M. EsxA and EsxB are secreted by an
1238 ESAT-6-like system that is required for the pathogenesis of Staphylococcus aureus infections.
1239 *Proc Natl Acad Sci U S A* **102**, 1169–74 (2005).
1240 79. Pratt, L. A. & Kolter, R. Genetic analysis of Escherichia coli biofilm formation: roles of flagella,
1241 motility, chemotaxis and type I pili. *Mol Microbiol* **30**, 285–293 (1998).
1242 80. Rodriguez-Rojas, A., Blazquez, J., Rodríguez-Rojas, A. & Blázquez, J. The Pseudomonas
1243 aeruginosa pfpI gene plays an antimutator role and provides general stress protection. *J*
1244 *Bacteriol* **191**, 844–850 (2009).
1245 81. March, S. C., Parikh, I. & Cuatrecasas, P. A simplified method for cyanogen bromide activation
1246 of agarose for affinity chromatography. *Anal Biochem* **60**, 149–152 (1974).
1247 82. O'Toole, G. A. & Kolter, R. Initiation of biofilm formation in Pseudomonas fluorescens WCS365
1248 proceeds via multiple, convergent signalling pathways: a genetic analysis. *Mol Microbiol* **28**,
1249 449–461 (1998).
1250 83. Lang, S., Livesley, M. A., Lambert, P. A., Littler, W. A. & Elliott, T. S. J. Identification of a novel
1251 antigen from Staphylococcus epidermidis. *FEMS Immunol Med Microbiol* **29**, 213–220 (2000).
1252 84. Clauditz, A., Resch, A., Wieland, K. P., Peschel, A. & Götz, F. Staphyloxanthin plays a role in the
1253 fitness of Staphylococcus aureus and its ability to cope with oxidative stress. *Infect Immun* **74**,
1254 4950–4953 (2006).
1255 85. Campbell, A. E. *et al.* Variable staphyloxanthin production by Staphylococcus aureus drives
1256 strain-dependent effects on diabetic wound-healing outcomes. *Cell Rep* **42**, 113281 (2023).
1257 86. Baracchi, D., Francese, S. & Turillazzi, S. Beyond the antipredatory defence: honey bee venom
1258 function as a component of social immunity. *Toxicon* **58**, 550–557 (2011).
1259 87. Terwilligert, T. C. & Eisenbergg, D. The structure of melittin. II. Interpretation of the structure.
1260 *Journal of Biological Chemistry* **257**, 6016–6022 (1982).
1261 88. Ownby, C. L., Powell, J. R., Jiang, M. S. & Fletcher, J. E. Melittin and phospholipase A2 from bee
1262 (Apis mellifera) venom cause necrosis of murine skeletal muscle in vivo. *Toxicon* **35**, 67–80
1263 (1997).
1264 89. Fennell, J. F., Shipman, W. H. & Cole, L. J. Antibacterial action of melittin, a polypeptide from
1265 bee venom. *Proc Soc Exp Biol Med* **127**, 707–710 (1968).
1266 90. Baracchi, D., Mazza, G. & Turillazzi, S. From individual to collective immunity: The role of the
1267 venom as antimicrobial agent in the Stenogastrinae wasp societies. *J Insect Physiol* **58**, 188–
1268 193 (2012).
1269 91. Cremer, S., Armitage, S. A. O. & Schmid-Hempel, P. Social immunity. *Curr Biol* **17**, (2007).
1270 92. Jones, C. J., Grotewold, N., Wozniak, D. J. & Gloag, E. S. Pseudomonas aeruginosa Initiates a
1271 Rapid and Specific Transcriptional Response during Surface Attachment. *J Bacteriol* **204**, (2022).
1272 93. Mukhi, M. & Vishwanathan, A. S. Beneficial Biofilms: a Minireview of Strategies To Enhance
1273 Biofilm Formation for Biotechnological Applications. *Appl Environ Microbiol* **88**, (2022).
1274 94. Kreve, S. & Reis, A. C. D. Bacterial adhesion to biomaterials: What regulates this attachment?
1275 A review. *Jpn Dent Sci Rev* **57**, 85–96 (2021).

95. Perez-Lopez, M. I. *et al.* Variations in carotenoid content and acyl chain composition in exponential, stationary and biofilm states of Staphylococcus aureus, and their influence on membrane biophysical properties. *Biochim Biophys Acta Biomembr* **1861**, 978–987 (2019).
96. Pratt, L. A. & Kolter, R. Genetic analysis of Escherichia coli biofilm formation: roles of flagella, motility, chemotaxis and type I pili. *Mol Microbiol* **30**, 285–293 (1998).
97. Rodriguez-Rojas, A., Blazquez, J., Rodríguez-Rojas, A. & Blázquez, J. The Pseudomonas aeruginosa pfpI gene plays an antimutator role and provides general stress protection. *J Bacteriol* **191**, 844–850 (2009).
98. Konrat, K. *et al.* The Bead Assay for Biofilms: A Quick, Easy and Robust Method for Testing Disinfectants. *PLoS One* **11**, (2016).
99. Belas, R. Biofilms, flagella, and mechanosensing of surfaces by bacteria. *Trends Microbiol* **22**, 517–27 (2014).
100. Ishihama, Y. *et al.* Protein abundance profiling of the Escherichia coli cytosol. *BMC Genomics* **9**, 102 (2008).
101. Blattner, F. R. *et al.* The complete genome sequence of Escherichia coli K-12. *Science* **277**, 1453–1462 (1997).
102. Baba, T. *et al.* Construction of Escherichia coli K-12 in-frame, single-gene knockout mutants: the Keio collection. *Mol Syst Biol* **2**, 2006 0008 (2006).
103. Stover, C. K. *et al.* Complete genome sequence of Pseudomonas aeruginosa PA01, an opportunistic pathogen. *Nature* **406**, 959–964 (2000).
104. Liberati, N. T. *et al.* An ordered, nonredundant library of Pseudomonas aeruginosa strain PA14 transposon insertion mutants. *Proc Natl Acad Sci U S A* **103**, 2833–2838 (2006).
105. Horsburgh, M. J. *et al.* sigmaB modulates virulence determinant expression and stress resistance: characterization of a functional rsbU strain derived from Staphylococcus aureus 8325-4. *J Bacteriol* **184**, 5457–67 (2002).
106. Yang, D. D. *et al.* Fitness and Productivity Increase with Ecotypic Diversity among Escherichia coli Strains That Coevolved in a Simple, Constant Environment. *Appl Environ Microbiol* **86**, (2020).
107. Dagert, M. & Ehrlich, S. D. Prolonged incubation in calcium chloride improves the competence of Escherichia coli cells. *Gene* **6**, 23–8 (1979).
108. O'Toole, G. A. & Kolter, R. Flagellar and twitching motility are necessary for Pseudomonas aeruginosa biofilm development. *Mol Microbiol* **30**, 295–304 (1998).
109. Moskowitz, S. M., Foster, J. M., Emerson, J. & Burns, J. L. Clinically Feasible Biofilm Susceptibility Assay for Isolates of Pseudomonas aeruginosa from Patients with Cystic Fibrosis. *J Clin Microbiol* **42**, 1915 (2004).
110. Boyles, J., Anderson, L. & Hutcherson, P. A new fixative for the preservation of actin filaments: fixation of pure actin filament pellets. *J Histochem Cytochem* **33**, 1116–1128 (1985).
111. March, S. C., Parikh, I. & Cuatrecasas, P. A simplified method for cyanogen bromide activation of agarose for affinity chromatography. *Anal Biochem* **60**, 149–152 (1974).
112. FRANK, L. H. & DEMOSS, R. D. On the biosynthesis of pyocyanine. *J Bacteriol* **77**, 776–782 (1959).
113. Lu, C. *et al.* How Hydrogel Stiffness Affects Adipogenic Differentiation of Mesenchymal Stem Cells under Controlled Morphology. *ACS Appl Bio Mater* **6**, 3441–3450 (2023).
114. Rappsilber, J., Mann, M. & Ishihama, Y. Protocol for micro-purification, enrichment, pre-fractionation and storage of peptides for proteomics using StageTips. *Nat Protoc* **2**, 1896–906 (2007).
115. Tyanova, S., Temu, T. & Cox, J. The MaxQuant computational platform for mass spectrometry-based shotgun proteomics. *Nat Protoc* **11**, 2301–2319 (2016).
116. Tyanova, S. *et al.* The Perseus computational platform for comprehensive analysis of (prote)omics data. *Nat Methods* **13**, 731–40 (2016).

117. R Core Team. *R: A Language and Environment for Statistical Computing.* (R Foundation for Statistical Computing, Vienna, Austria, 2022).

Supplementary information

Cross-linked agarose-gelatine beads as a substrate for investigating biofilms of bacterial pathogens

Dan Roizman[1§], Maren Herzog[1§], Arpita Nath[1], Nivetha Pachaimuthu[2], Ahmad Hujeirat[1], Benno Kuropka[3], Jens Rolff[1*], and Alexandro Rodríguez-Rojas[1,2*]

[1]Evolutionary Biology, Institut für Biologie, Freie Universität Berlin, Berlin, Germany.

[2]Small Animal Internal Medicine, Clinic for Small Animals, University of Veterinary Medicine, Vienna, Austria.

[3]Institute of Chemistry and Biochemistry, Freie Universität Berlin, Berlin, Germany.

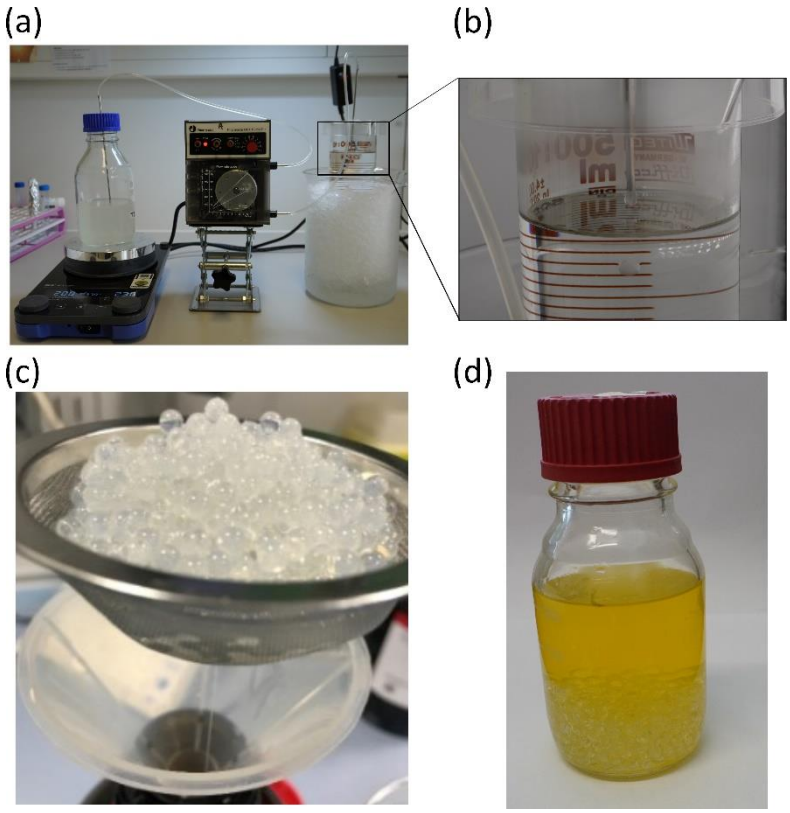

Fig. S1. Production process for the agarose-gelatine beads. (A) The bead substrate is carefully placed on a heating plate, with continuous stirring, ensuring the temperature and that the bottle stands higher than the pump and the collection vessel in the ice container. (B) Droplets form at the end of the metal tube following the peristaltic movement rate. The beads gain their spherical form due to hydrogel surface tension, a magnitude drop in temperature, and the inert oil's hydrophobic environment. (C) The resulting beads are sieved and washed with tap water until it flows transparent, with a household detergent added to the first wash to enhance the displacement of oil molecules. The mineral oil is filtered for reuse. The beads are then ready for the following cross-linking steps. (D) The resulting beads, in the medium of choice following autoclaving, can be stored for at least several months at 4°C as necessary.

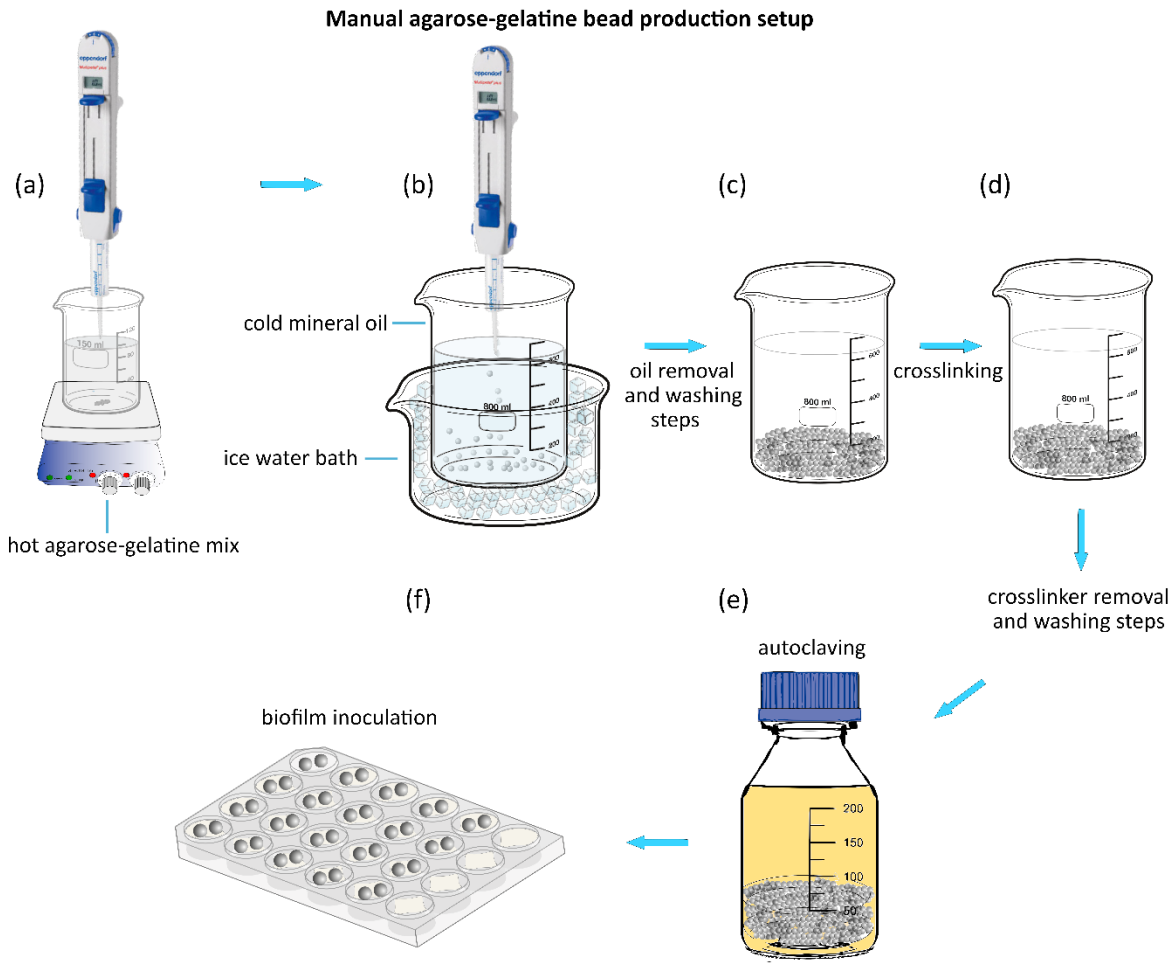

Fig. S2. This figure illustrates a more accessible setup for bead production using a multi-step pipette instead of a peristaltic pump, as shown in Fig. 1. In the initial step (a), a fused mixture of gelatine-agarose (2% each in distilled water) is prepared and placed on a magnetic stirrer with a hot plate to maintain liquidity. This solution is continuously added to ice-cold mineral oil using a multi-step pipette to maintain the size and consistency of the beads, followed by the same steps as described in Fig. 1. In step (b), the mineral oil is removed, and washing steps, including the use of detergent, are performed to eliminate oil residues. Following this, in step (c), the beads undergo crosslinking using divinyl sulfone (DVS), with the crosslinker later removed through additional washing steps. After removing the crosslinker, the beads are transferred to a bottle and autoclaved at 121°C for 15 minutes at 1 atmosphere (d), a critical step that ensures the long shelf life of the beads. Once autoclaved, the beads can be stored for several months until use. In the final step (e), the beads are transferred to a 24-well multiwell plate, where the chosen bacteria are inoculated, and the biofilm is established, as previously described. For additional details, see the Materials and Methods section.

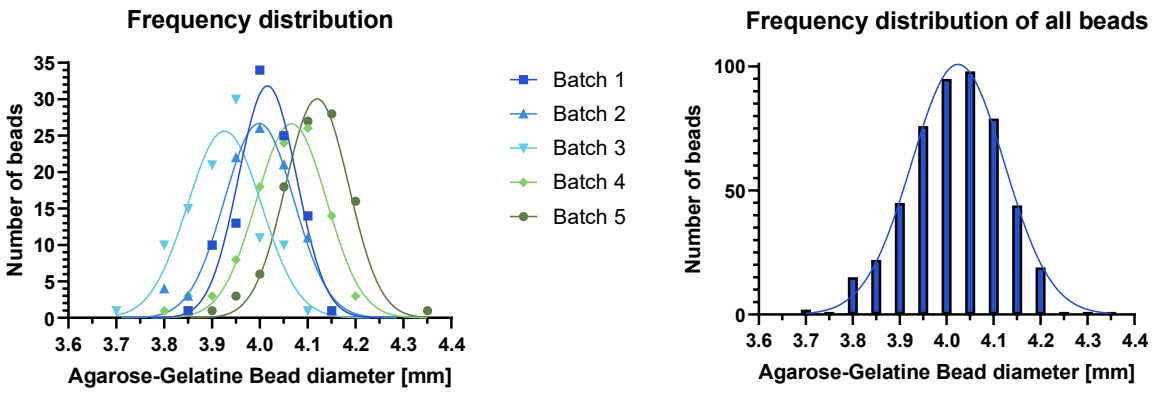

Fig. S3. Statistical validation of the consistent size distribution of five independent batches of agarose-gelatine bead random samples (N=100). (A) 99% of the populations of beads in each batch consistently follow a normal distribution as per the D'Agostino & Pearson test with *p*-values above α=0.05. The data plotted here as the number of beads per 0.05 mm for simplification purposes. Means range between 4.11-3.92 mm with standard deviations below 0.08 mm. The frequency distribution of the whole sampled population of agarose-gelatine beads (B) 99% of produced beads follow a normal distribution as represented by the Gaussian curve (B).

Supplementary protocol I

Agarose-gelatine beads production protocol

Introduction: This protocol describes the procedure for producing agarose-gelatine beads (AGBs) as a substrate for various applications in biotechnology and microbiology. Due to their mechanical and thermal stability, AGBs offer a stable matrix for immobilising enzymes, cells, or other biomolecules. The protocol includes steps for bead production, crosslinking to enhance stability, and deactivation to remove residual reactants.

Materials:

- Agarose
- Gelatine
- Distilled water
- Inert mineral oil
- Vacuum pump
- Peristaltic pump
- Silicone tubes
- Metal tubes
- 0.5 M sodium carbonate buffer
- Sodium hydroxide
- Divinyl sulphone (DVS)
- 2-Mercaptoethanol
- Glycine
- Sodium chloride
- Parafilm
- Aluminium foil
- Shaker

Procedure:

1. Production of Agarose-gelatine Beads:

1.1. In a 400 mL bottle, dissolve 4 g each of agarose and gelatine in 200 mL of cold distilled water.
1.2. Autoclave the solution for 20 minutes at 121°C and 2.1 bar absolute pressure.
1.3. Maintain the liquid substrate at 60°C on a hot plate stirrer throughout production.
1.4. Prepare a 1 L glass beaker filled with approximately 500 mL of inert oil as a collection vessel.
1.5. Remove air bubbles from the substrate using a vacuum pump if necessary.
1.6. Cool the collection vessel in a bucket ice water container bath.
1.7. Connect a peristaltic pump and calibrate the flow rate to deliver approximately 40 µl drops, which can be empirically determined using an analytical scale. Perform some adjustments by measuring 10 to 20 beads to reach the desired size.
1.8. Use silicone and metal tubes to deliver uniform drops of the agarose-gelatine mixture into the cooled inert oil. Place the tube approximately 1 to 2 cm from the oil's surface.
1.9. The drops tend to solidify immediately, forming ~4 mm AGBs.
1.10. Sieve and wash the beads with tap water until it runs transparent, filtering and reusing the mineral oil.

2. Crosslinking of agarose-gelatine beads:

2.1. Weigh the washed beads to calculate the required amount of DVS (0.5% v/w).
2.2. Cover the beads with approximately 550 mL of 0.5 M sodium carbonate buffer adjusted to pH 11.0 using sodium hydroxide 1 N.
2.3. Add 1.25 mL of the DVS solution per 250 g of wet gel beads in the buffer.
2.4. Allow the crosslinking reaction to proceed overnight on a shaker at room temperature, covering the containing flask with parafilm to prevent evaporation.
2.5. The next day, wash the beads with distilled water by decanting and sieving until they have a neutral pH. Between washes, allow the beads to rest for at least 10 minutes.

3. Crosslinking reaction stop and crosslinker removal:

3.1. Mix the wet gel beads with 0.01 mL of 2-Mercaptoethanol per mL of bead suspension in a neutral or slightly alkaline medium.
3.2. Cover the reaction vessel with parafilm to avoid evaporation and aluminium foil to avoid light exposure.
3.3. Allow the reaction to proceed overnight on a shaker at room temperature.
3.4. Discard excess solution and wash beads several times with distilled water.
3.5. Suspend beads in a glycine solution (10% w/v in 1 M sodium carbonate buffer, pH 10.0).
3.6. Allow the reaction to proceed overnight on a shaker at room temperature.
3.7. Wash beads three times with 0.1 M carbonate-bicarbonate buffer (pH 10.0) and then 0.1 M citrate buffer (pH 4.0) with sodium chloride.
3.8. Autoclave beads with media such as LB or Mueller-Hinton broth at 4°C for long-term storage.

Supplementary protocol II

Protocol for cultivating biofilms on agarose-gelatine beads:

Introduction: This protocol provides a method for cultivating biofilms on agarose-gelatine beads (AGBs) for downstream applications such as antibiofilm agent treatments, microscopy, and cell recovery. AGBs provide a stable matrix for biofilm formation and can be used with various bacterial species and growth media.

Materials:
- Autoclaved agarose-gelatine beads
- Medium of choice
- 24-well microplate (preferably polypropylene)
- Bacteria culture
- 0.9% NaCl saline solution
- Vacuum aspirator
- Orbital shaker
- 1 ml pipette and tips

Procedure:
1. Prepare overnight cultures of the bacteria of choice in the medium of choice.
2. Dilute the overnight culture to achieve an inoculum of approximately 10^6 colony-forming units (CFU) per millilitre.
3. Add 1 ml of the diluted bacterial culture to each microplate well containing the agarose-gelatine beads and medium.
4. Place two autoclaved agarose-gelatine beads in each well of a 24-well microplate.
5. Place the microplate in an orbital shaker and incubate at 37°C with moderate shaking (20 to 30 rpm).
6. Incubate for 24 to 94 hours, depending on the biofilm's desired maturity and the bacteria's growth speed.
7. If required, perform daily washings to remove planktonic cells and maintain the biofilm by removing the planktonic phase with a 1 ml pipette. Wash the biofilm-containing beads by performing three consecutive washes by gentle addition and removal of with 0.9% NaCl saline solution using a 1 ml pipette. Use a vacuum aspirator for better results.
8. After the desired incubation period, wash the beads as indicated in step 7 and transfer the biofilm-containing beads to a fresh microplate for downstream applications such as antibiofilm agent treatments, microscopy, and cell recovery.

Supplementary protocol III

Protocol for extracting viable bacteria from agarose-gelatine beads biofilms.

Introduction: This protocol is a refined method for extracting viable bacteria from biofilm on the surface of agarose-gelatine beads. It includes an additional step of digestion with DNAase I and RNAse A, followed by the addition of papain and mild sonication to digest the extracellular matrix. The protocol allows the determination of anti-biofilm treatment or simplifies the enumeration of bacteria within the biofilm.

Materials:

Biofilm-forming bacteria (e.g., *Staphylococcus aureus*, *Escherichia coli*, *Pseudomonas aeruginosa* etc)
Sterile agarose-gelatine beads for biofilm culture

- Digestion buffer (150 mM NaCl, 50 mM Tris-buffer, 10 mM $MgCl_2$, 5 mM L-cysteine, 5 mg/ml DNAse I, 2 mg/ml RNAse A, pH 7.5).
- Papain stock solution 10 mg/ml
- 2 ml microcentrifuge tubes
- Microcentrifuge
- Sonicator bath

Procedure:

1. Cultivate biofilm-forming bacteria in agarose-gelatine beads according to Supplementary Protocol II under biofilm-inducing conditions until mature biofilms are formed, including those subjected to a chosen treatment (e.g., antimicrobial treatment).
2. Following bead culture, wash the beads with 0.9% NaCl solution.
3. Transfer two beads from each well of the 24-well microplates into separate 2 ml microcentrifuge tubes.
4. Add 200 µl of digestion buffer (150 mM NaCl, 50 mM Tris-buffered saline (TBS) at pH 7.5, 10 mM $MgCl_2$, 5 mM L-cysteine, 5 mg/ml DNAse I, and 2 mg/ml RNAse A) to each microcentrifuge tube.
5. Incubate the tubes for 15 minutes at 37°C in a thermo block or recirculating water bath, moderately shaking intermittently to promote thorough enzymatic digestion.
6. After enzymatic digestion, add 20 µl of papain stock solution (10 mg/ml) to each tube, achieving a final concentration of approximately 500 µg/ml. Submerge the tubes in a pre-warmed sonication bath and sonicate for 5 minutes to further disrupt the biofilm matrix.
7. Transfer the supernatant containing the solubilised biofilm components to fresh tubes. Wash the beads once with 1 ml of digestion buffer, then combine the wash with the previously collected supernatant to ensure maximal recovery of biofilm material.
8. Centrifuge the combined suspension at 10,000 × g for 5 minutes to pellet bacterial cells and any remaining debris.
9. Discard the supernatant and carefully resuspend the bacterial pellet in 1 ml of 0.9% NaCl solution.
10. Plate appropriate dilutions of the resuspended bacterial suspension on selective media of choice to determine the colony-forming unit (CFU) count, facilitating subsequent experimental procedures using the recovered bacteria.

Supplementary protocol IV

Protocol for preparation of bacterial cell lysate for proteomics (LC-MS) from agarose-gelatine bead biofilms by freeze-thaw cycles.

Introduction:

This protocol describes a method for preparing bacterial cell lysate suitable for proteomic analysis using liquid chromatography-mass spectrometry (LC-MS) from biofilms grown on agarose beads. The protocol involves treating the biofilm-containing agarose beads with desired conditions, followed by freeze-thaw cycles to lyse the cells and extract proteins. The resulting lysate can be used for downstream proteomic analysis to characterise the bacterial proteome.

Materials:

- Agarose-gelatin bead biofilm samples
- Dry ice or liquid nitrogen
- Water bath set to 37°C
- Microfuge tubes
- Microfuge
- Vacuum concentrator machine
- HEPES buffer: 1M solution
- 50 mM buffer Ammonium Bicarbonate (ABC). Always use a freshly made solution.
- 55 mM Iodoacetamide solution. The solution should be freshly made and protected from light.
- Dithiothreitol (DTT) 1 M stock solution freshly made.
- Urea buffer (6 M urea, 2 M thiourea, and 10 mM HEPES, pH 8.0).
- Buffer A (5% Acetonitrile, 0.3% Trifluoroacetic acid). Always use a freshly made solution.
- Buffer B (80% Acetonitrile, 0.3% Trifluoroacetic acid). Always use a freshly made solution.

Procedure:

1. Prepare biofilm-containing agarose beads according to the desired experimental conditions following Supplementary Protocol II. Use at least five replicas per experimental condition, including a control group.
2. Wash the beads with 0.9% NaCl solution following the bead culture.
3. Transfer two beads from each well of the 24-well multiwell plates into separate 1.5 ml microcentrifuge tubes.
4. Add 200 µl of urea buffer (6 M urea, 2 M thiourea, 10 mM HEPES, pH 8.0) to each microcentrifuge tube.
5. Freeze the samples on dry ice or liquid nitrogen and leave for at least 2 minutes. Thaw immediately at 37°C in a nearby water bath. Mix well by flicking the tubes to ensure complete dissolution of urea. Repeat the freeze-thaw process for four more cycles (5 cycles in total).
6. Centrifuge the combined suspension at 10,000 × g for 10 minutes to pellet bacterial debris and agarose beads.
7. Carefully collect 100 µl from each tube without disturbing the pellet, transfer it to a fresh tube, and place it on ice.
8. Use 10 µl of the cell lysate to determine total protein concentration using an appropriate method (Biuret, BCA, or similar).
9. Use approximately 50 µg of total protein for mass spectrometry sample preparation.

Protein in-solution digestion for mass spectrometry:

1. Adjust the final volume of the tubes containing the 50 µg of total protein to 50 µl using urea buffer to reach a final protein concentration of 1 mg/ml.
2. Add 2.5 µl of DTT 10 mM solution (see buffers and solutions section) to each tube containing 50 µl of protein solution and incubate for 30 mins at room temperature.

3. Add 2.5 µl of 55 mM iodoacetamide solution to each tube and incubate for 30 min at room temperature in the dark.
4. Dilute samples with 4 volumes of ABC (final urea concentration should be below 2 M) by adding 200 µl of ABC buffer.
5. Add 2 µl of 0.5 µg/µl trypsin (sequencing grade) and incubate overnight at room temperature.
6. Stop trypsin digestion by adding 8 µl of 10% TFA to each sample (the final concentration will be approximately 0.3%) and mixing well by pipetting.
7. Add 14 µl of acetonitrile to each tube (final concentration will be approximately 5%).
8. Proceed with peptide desalting and purification using the StageTip procedure. Digested peptides can also be stored at -20°C until use.

StageTip for peptide desalting and purification:

1. Prepare the 200 µl tips (without filter) for peptide binding and micropurification upon digestion of the protein sample (so-called StageTips). One tip will be used per sample. Label each tip according to the sample code. Using a puncture device such as a biopsy punch to cut and stack two disks inside 200 µl (see Figure 1 for reference).
2. Using an awl, make a hole in the cap of a 2 ml microcentrifuge tube (Eppendorf-type) with a diameter slightly smaller than the broadest part of the pipette tip. Place a tip containing the C18 membrane disks into the 2 ml plastic tube (Eppendorf-type). This tube will be the holder and collecting reservoir for the tips (see Figure 1 for reference).
3. Add 100 µl of methanol (LC-MS grade) to activate each tip.
4. Centrifuge the tip-carrying tubes for 10 seconds at 10,000 g and check that some methanol is retained on the matrix disks. If all solvent goes through, replace the tip with a new one and repeat the procedure. This ensures that the c18 membrane is tightly packed inside the tip.
5. Spin the tip-carrying tubes for 15 seconds at 3,000 x g to remove all methanol.
6. Equilibrate the tips by adding 200 µl of Buffer A and centrifuge at 3,000 g for 5 minutes at room temperature.
7. Spin the tip-carrying tubes at 3,000 g to remove Buffer A. Proceed as soon as possible to the next step to prevent the matrix from drying.
8. Add the acidified samples to their corresponding tips and centrifuge at 3,000 g for 5 minutes at room temperature.
9. Wash the tips by adding 200 µl of Buffer A and centrifuge at 3,000 g for 5 minutes at room temperature.
10. Place the tip into a tip rack and store at +4°C until the desired time for elution and analysis. The samples can be stored for up to three months under these conditions.
11. For sample elution, add 100 µl of Buffer B to each tip and place them in the collection tubes.

12. Evaporate the solvent by vacuum centrifugation and resuspend the peptides in an appropriate volume of the buffer suitable for liquid chromatography-mass spectrometry (LC-MS), e.g., 20 µl of 4 % Acetonitrile and 0.05 % Trifluoroacetic acid.

Notes:

- Prolonged storage of digested proteins in plastic tubes may result in irreversible loss of peptides due to binding to the tubes' walls.
- Wear gloves during the procedure to avoid sample contamination from the operator's epithelial cells and to prevent toxicity or irritation caused by some reagents when they come into contact with the skin.
- All solutions used in this protocol should be freshly made before execution as indicated.
- The use of DTT is intended to reduce disulfide bonds and enhance the chance of detecting peptides containing cysteine.
- Iodoacetamide alkylates free thiols of cysteine residues, preventing the re-formation of disulfide bonds. Please consider carbamidomethyl on cysteine as a fixed modification during the database search.

Supplementary protocol V

Protocol for staining and quantifying bacterial biofilm production using a crystal violet stain.

Materials:
- Agarose-gelatine bead biofilm samples and controls
- Medium of choice
- 24-well microplate (preferably polypropylene)
- 96-well microplate
- 0.9% NaCl saline solution
- Crystal violet stock solution (from Gram-stain kit)
- 95% Ethanol solution
- Triton X-100 solution
- Orbital shaker
- 1 ml pipette and tips
- Spectrophotometer for absorbance measurement

1. Cultivate biofilm-forming bacteria on agarose-gelatine beads or any other material according to Supplementary Protocol II under biofilm-inducing conditions until mature biofilms are formed, including fresh, uninoculated beads as control. Use some beads without inoculation as a blank control.
2. Following bead culture, gently wash the beads twice with 0.9% NaCl solution.
3. If necessary, transfer to a new 24-well microplate and stain bead biofilm samples with 0.05% Crystal violet in 0.9% NaCl solution, 1 ml per well, for 1 min.

4. Aspire and discard the staining solution using a pipette or a vacuum aspirator.
5. Rinsed the beads several times with preheated (at 45 C) dH2O2 tap water to allow the interspecifically bound crystal violet to diffuse from the internal areas of the beads. Allow the beads to rest in an incubator for 10 minutes until no visible colour is present in the control blank beads. Remove the wash and allow the beads to dry at room temperature for 10 minutes.
6. Solubilize the remaining crystal violet from the beads by adding 1 ml 95% Ethanol containing 0.05% (w/v) Triton X-100 and incubate at 45°C for 30 minutes on an orbital shaker at room temperature.
7. Transfer 200 µl samples per well of a 96-well microplate and measure optical density at 590 nm using a plate reader or an equivalent machine.

Notes:

- Crystal violet dye is toxic and potentially carcinogenic. Use gloves, a lab coat and eye protection.
- A flexible piece of mesh can be used as a sieve during intensive steps, such as washing with tap water, to ensure the beads retain their position and remain in their corresponding well.
- This method with AGB has a relatively high background due to the diffusion of crystal violet dye to the inner part of the bead hydrogel.